2. Natural Time. Background

Abstract. Time and not space poses the greatest challenge to science. Conventional time is modeled as the one-dimensional continuum $\mathscr{R}$ of real numbers. This continuity, however, does *not* stem from *any* fundamental principle. On the other hand, natural time χ, which is a new time domain introduced by the authors in 2001, is *not* continuous and its values as well as those of the energy form *countable* sets. Novel dynamical features hidden behind time series in complex systems can emerge upon analyzing them in natural time, which conforms to the desire to reduce uncertainty and extract signal information as much as possible. The fluctuations, under time reversal, of the natural time can serve in time series for the quantification of the long-range dependence. Natural time analysis also enables the study of the dynamical evolution of a complex system and identifies *when the system enters a critical state*. In particular, the normalized power spectrum $\Pi(\omega)$ is introduced in natural time, and its Taylor expansion leads, at low natural (cyclic) frequencies ω ($\omega \to 0$), to the expression $\Pi(\omega) \approx 1 - \kappa_1 \omega^2$. The values of the coefficient κ_1, which is just the variance of natural time, i.e., $\kappa_1 = \langle \chi^2 \rangle - \langle \chi \rangle^2$, are useful in identifying the approach to a critical point such as SES whose κ_1 value is shown to be 0.070. In addition, natural time analysis enables the distinction between the two origins of self-similarity, i.e., whether self-similarity solely results from long-range temporal correlations (the process's memory only) or solely from the process's increments' infinite variance (heavy tails in their distribution). In general, however, the self-similarity may result from both these origins, a case that can be also identified by natural time.

2.1 Introduction to natural time

In this Section, we follow Ref. [50]. In reviewing the state of physics today, a consensus seems to emerge that we are missing something absolutely fundamental, e.g., Refs. [2, 17]. Furthermore, there is a widespread belief that, it is not space but time that in the end poses the greatest challenge to science (e.g., p. 18 of Ref. [71]) as it will be further discussed in the next subsection.

P.A. Varotsos et al., *Natural Time Analysis: The New View of Time: Precursory Seismic Electric Signals, Earthquakes and other Complex Time Series*, Springer Praxis Books, DOI 10.1007/978-3-642-16449-1_2,

2.1.1 Time and not space poses the greatest challenge to science

Time, according to Weyl (see p. 5 of Ref. [67]) for example, is "the primitive form of the stream of consciousness. It is a fact, however, obscure and perplexing to our minds, that ... one does not say this *is* but this is *now*, yet no more" or according to Gödel "that mysterious and seemingly self-contradictory being which, on the other hand, seems to form the basis of the world's and our own existence" (p. 111 of Ref. [71]). The challenge seems to stem from the fact that special relativity and quantum mechanics, which are the two great (and successful) theories of twentieth-century physics, are based on entirely different ideas, which are not easy to reconcile. (In general, the former theory, according to Einstein [10], is an example of "principled theory" in the sense that you start with the principles that underlie the theory and then work down to deduce the facts, while the latter is a "constructive theory" meaning that it describes phenomena based on some known facts but an underlying principle to explain the strangeness of the quantum world has not yet been found.) In particular, special relativity puts space and time on the *same* footing, but quantum mechanics treats them very differently, e.g., see p. 858 of Ref. [69]. (In quantum gravity, space is fluctuating and time is hard to define, e.g., Ref. [70].) More precisely, as far as the theory of special relativity is concerned, let us recall the following wording of Einstein [11]:

"Later, H. Minkowski found a particularly elegant and suggestive expression ..., which reveals a formal relationship between Euclidean geometry of three dimensions and the space time *continuum* of physics ... . From this it follows that, in respect to its *rôle* in the equations of physics, though not with regard to its physical significance, time is equivalent to the space co-ordinates (apart from the relations of reality). From this point of view, physics is, as it were, Euclidean geometry of four dimensions, or, more correctly, a statics in a four-dimensional Euclidean *continuum*." – whereas in quantum mechanics, Von Neumann complains [28]:

"First of all we must admit that this objection points at an essential weakness which is, in fact, the *chief weakness* of quantum mechanics: its non-relativistic character, which distinguishes the time t from the three space coordinates x, y, z, and presupposes an objective simultaneity concept. In fact, while all other quantities (especially those x, y, z, closely connected with t by the Lorentz transformation) are represented by operators, there corresponds to the time an ordinary number-parameter t, just as in classical mechanics."

Note also that Pauli [33] has earlier shown that there is no operator canonically conjugate to the Hamiltonian, if the latter is bounded from below. This means that for many systems a time operator does *not* exist. In other words, the introduction of an operator t is basically forbidden and the time must necessarily be considered as an ordinary number (but recall the long-standing question that Schrödinger's equation, as well as Einstein's general theory of relativity, is symmetric under time reversal in contrast to the fact that our world is *not*, e.g., Ref. [35]). These observations have led to a quite extensive literature mainly focused on time-energy (as well as on "phase-action") uncertainty relation, proposing a variety of attempts to overcome these obstacles. The discussion of this literature, however, lies beyond the scope of the present monograph. We just summarize here that the (conventional) time t is *currently* modeled as the one-dimensional *continuum* $\mathbb{R}$ of the real numbers, e.g., p. 10 of Ref. [70] (or p. 12 of Ref. [67] in which it is stated that

"... the straight line ... is homogeneous and a linear *continuum* just like time"). It is the consequences of this *continuity* that will be compared to the newly introduced concept of natural time, in a sense that will be discussed later in Section 2.7.

2.1.2 Definition of natural time

In a time series comprising N events, the *natural time*

$$\chi_k = k/N \tag{2.1}$$

serves as an index for the *occurrence* of the k-th event [51, 52], and it is smaller than, or equal to, unity (note that the symbol χ originates from the ancient Greek word $\chi\rho\acute{o}\nu o\varsigma$ (chronos), see the cover page, which means "time").

In natural time analysis the evolution of the pair of two quantities (χ_k, Q_k) is considered, where $\chi_k = k/N$, N being the total number of events, and Q_k denotes in general a quantity proportional to the energy of the individual (k-th) event [51, 52]. Equivalently with Q_k, one can consider the quantity

$$p_k = \frac{Q_k}{\sum_{n=1}^{N} Q_n}, \tag{2.2}$$

$$\sum_{k=1}^{N} p_k = 1, \tag{2.3}$$

where p_k is the *normalized* energy emitted during the k-th event. In other words, the evolution of the pair either (χ_k, Q_k) or (χ_k, p_k) is considered in natural time analysis.

For example, to perform the analysis of dichotomous electric signals (Fig. 2.1(a)), which is frequently the case of a SES activity (see Chapter 1), we consider Q_k as being proportional to the duration of the k-th pulse [51, 52, 55, 54]. As another example, we refer to the analysis of seismic events (Fig. 2.1(b)): we then consider the evolution of the pair (χ_k, M_{0_k}) where M_{0_k} stands for the seismic moment of the k-th earthquake [51, 53, 61, 60], since M_{0_k} is proportional to the energy emitted in that earthquake (note that M_{0_k} differs essentially from the magnitude M, but they are interconnected [21] $\mathrm{M}_{0_k} \propto 10^{c\mathrm{M}}$ where $c \approx 1.5$, see also Section 6.1). Other examples elaborated in this monograph are: first, the analysis of electrocardiograms (see Fig. 2.2) which will be discussed in detail in Chapter 9. Second, the case of long-duration SES activities of non-obvious dichotomous nature, which is treated in Section 4.11. Third, the analysis of various dynamical models (among which a case of quasi-periodic Q_k, see Fig.(8.4)) in natural time which is discussed in detail in Chapter 8.

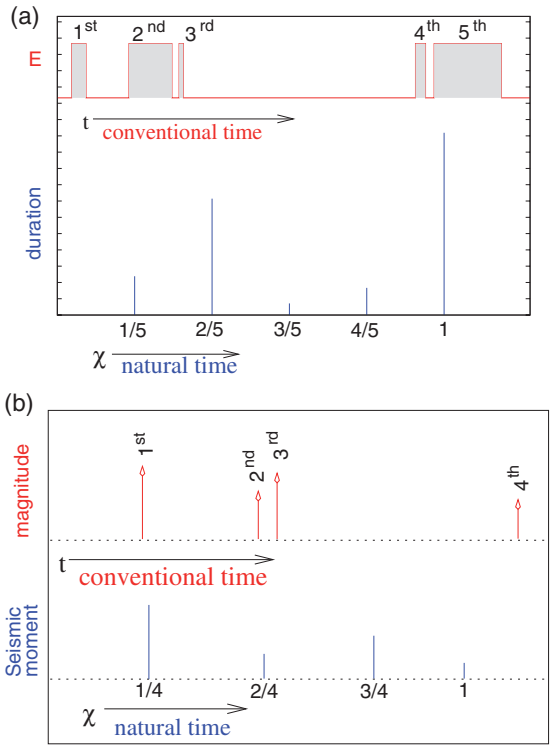

Fig. 2.1 (a) How a dichotomous series of electric pulses in conventional time t (upper panel, red) can be read in natural time χ (lower panel, blue). The symbol E stands for the electric field. (b) The same as in (a), but for a series of seismic events.

2.1.3 The "uniform" distribution

Among the various applications of natural time that will be discussed throughout this monograph, there is the fundamental paradigm of the "uniform" distribution that corresponds for example to the case when the system under study is in a stationary state emitting uncorrelated bursts of energy:

As a "uniform" distribution we consider the case when Q_k are *positive independent and identically distributed* (p.i.i.d.) random variables.

In this case, the expectation value $\mathscr{E}(p_k)$ of the point probabilities p_k is $\mathscr{E}(p_k) = 1/N$ by virtue of Eq. (2.3).

Let us now consider the distribution

$$p(\chi) = \sum_{k=1}^{N} p_k \delta(\chi - \chi_k) = \sum_{k=1}^{N} p_k \delta\left(\chi - \frac{k}{N}\right) \tag{2.4}$$

that corresponds to the point probabilities p_k. (Note that, $\delta(x)$ stands for the usual Dirac delta function.)

As $N \to \infty$, $p(\chi)$ for a "uniform" distribution tends to

$$p(\chi) = 1, \tag{2.5}$$

leading to an average value of natural time

$$\langle \chi \rangle = \int_0^1 \chi p(\chi)\, \mathrm{d}\chi = \frac{1}{2}. \tag{2.6}$$

2.2 Time reversal and natural time

In a time series comprising N events, the effect of the time-reversal operator $\hat{T}$ on Q_k is given by

$$\hat{T} Q_k = Q_{N-k+1}, \tag{2.7}$$

so that the first pulse $(k = 1)$ is positioned last in the time reversed time-series, the second becomes last but one, etc.

Thus, the time reversal operator $\hat{T}$ in natural time acting on p_k results in

$$\hat{T} p_k = p_{N-k+1} \tag{2.8}$$

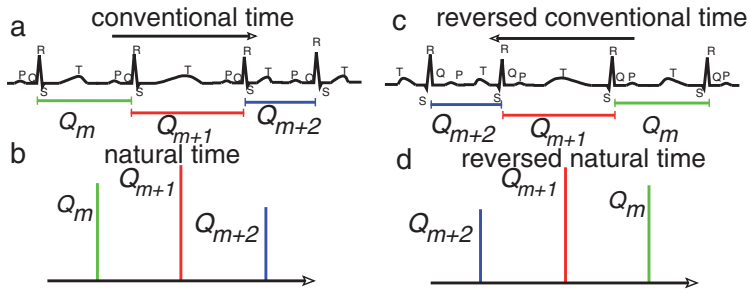

Fig. 2.2 (a) Schematic diagram (not to scale) of a four heartbeat excerpt of an ECG (for the notation of the inflection points see § 9.1.1) in the usual (conventional) time domain. The durations Q_m, Q_{m+1}, Q_{m+2} of the three RR intervals are shown. (b) The RR interval time series of (a) read in natural time; the vertical bars are equally spaced, but the length of each bar denotes the duration of the corresponding RR interval marked in (a). In (c) and (d) we depict (a) and (b), respectively, but under time reversal. Reprinted with permission from Ref. [57]. Copyright (2007), American Institute of Physics.

Let us consider an example from the case of electrocardiogram (ECG) analysis discussed in detail in Chapter 9. Figure 2.2(a) provides a schematic diagram of a four-heartbeat excerpt of an ECG in the conventional time domain. The durations Q_m, Q_{m+1} and Q_{m+2} of the three RR (beat to beat) intervals are marked in green, red and blue, respectively. In Fig. 2.2(b), we show how the RR interval time series of Fig. 2.2(a) is read in natural time: the vertical bars are *equally* spaced and the length of each bar denotes the duration of the corresponding RR interval marked in Fig. 2.2(a). We now turn to the effect of the time reversal: Fig. 2.2(c) depicts how the four heartbeat excerpt of Fig. 2.2(a) becomes upon reversing the conventional time (thus the sequential order of colors–durations in Fig. 2.2(a) has been reversed) and Fig. 2.2(b) turns to Fig. 2.2(d). Time reversal may reveal important elements of the dynamics of the system as will become clear, for example, in identifying the occurrence time of an impending cardiac arrest; see § 9.4.1.

2.2.1 Interconnection of the average value of natural time with the effect of a small linear trend on a "uniform" distribution

The way through which natural time captures the influence of the effect of a small linear trend on a "uniform" distribution is studied on the basis [60, 58] of the parametric family of probability density functions (cf. Eq. (2.5)):

$$p(\chi;\varepsilon) = 1 + \varepsilon(\chi - 1/2), \tag{2.9}$$

where the parameter ε quantifies the linear trend. Such a family of pdfs shares the interesting property

$$\hat{T}\, p(\chi;\varepsilon) = p(\chi;-\varepsilon), \tag{2.10}$$

i.e, the action of the time reversal is obtained by simply changing the sign of ε. A *linear* measure of ε in natural time is [58] the average of the natural time itself since:

$$\langle \chi \rangle = \int_0^1 \chi p(\chi;\varepsilon)\, \mathrm{d}\chi = \frac{1}{2} + \frac{\varepsilon}{12}. \tag{2.11}$$

In the following subsection, we shall show that if we consider the fluctuations of this simple measure upon time reversal, we can obtain information on the long-range dependence of Q_k.

2.2.2 Quantification of the long-range dependence from the fluctuations of the average value of natural time under time reversal

As discussed in § 1.4.1, in order to study the long-range dependence in a time series, e.g., Q_k, we have to define a scale-dependent measure (for example, $F(s)$ of Eq. (1.12) constitutes such a measure in DFA; see § 1.4.2).

We shall show that such a scale-dependent measure is the one that quantifies how the average value of natural time fluctuates upon time reversal when considering a window of length l (= number of) consecutive events sliding through the time series Q_k.

In a window of length l starting from Q_{m_0} (thus ending at Q_{m_0+l-1}), the values of natural time are $\chi_k = k/l$ for $k = 1,2,\ldots,l$ and correspond to the point probabilities $p_k = Q_{m_0+k-1}/\sum_{i=1}^{l} Q_{m_0+i-1}$. Since under time reversal we have $\hat{T}p_k = p_{l-k+1}$, the fluctuations of the average value of natural time under time reversal could be quantified by

$$\Delta\chi_l^2 \equiv \mathscr{E}[(\langle\chi\rangle - \langle\hat{T}\chi\rangle)^2] = \mathscr{E}\left\{\left[\sum_{k=1}^{l}\frac{k}{l}(p_k - p_{l-k+1})\right]^2\right\}, \tag{2.12}$$

where the symbol $\mathscr{E}[\ldots]$ denotes the expectation value obtained when a window of length l is sliding through the time series Q_k. The evaluation of $\mathscr{E}[\ldots]$ can be carried out either by full computation or by Monte Carlo; the full computation refers to the case when the window is sliding consecutively event by event, i.e., m_0 takes all the $N-l+1$ ($m_0 = 1,2,\ldots N-l+1$) possible values, whereas in Monte Carlo evaluation m_0 is selected randomly. The argument of $\mathscr{E}[\ldots]$ is computed by substituting $p_k = Q_{m_0+k-1}/\sum_{i=1}^{l} Q_{m_0+i-1}$ and $p_{l-k+1} = Q_{m_0+l-k}/\sum_{i=1}^{l} Q_{m_0+i-1}$. The sum of the resulting values over the number of the selected segments (different m_0) is assigned to $\mathscr{E}[\ldots]$.

By expanding the square in the last part of Eq. (2.12), we obtain

$$\Delta\chi_l^2 = \sum_{k=1}^{l}\left(\frac{k}{l}\right)^2 \mathscr{E}[(p_k - p_{l-k+1})^2] + \sum_{k\neq m}\frac{km}{l^2}\mathscr{E}[(p_k - p_{l-k+1})(p_m - p_{l-m+1})]. \tag{2.13}$$

Equation (2.3) constitutes the basic relation that interrelates p_k, i.e., $\sum_{k=1}^{l} p_k = 1$ or equivalently $p_k = 1 - \sum_{m\neq k} p_m$. By subtracting from the last expression its value for $k = l-k+1$, we obtain $p_k - p_{l-k+1} = -\sum_{m\neq k}(p_m - p_{l-m+1})$, and hence

$$(p_k - p_{l-k+1})^2 = -\sum_{m\neq k}(p_k - p_{l-k+1})(p_m - p_{l-m+1}). \tag{2.14}$$

By substituting Eq. (2.14) into Eq. (2.13), we obtain

$$\begin{aligned}\Delta\chi_l^2 = &-\sum_{k=1}^{l}\left(\frac{k}{l}\right)^2 \sum_{m\neq k}\mathscr{E}[(p_k - p_{l-k+1})(p_m - p_{l-m+1})] \\ &+ \sum_{k\neq m}\frac{km}{l^2}\mathscr{E}[(p_k - p_{l-k+1})(p_m - p_{l-m+1})]\end{aligned} \tag{2.15}$$

which simplifies to

$$\Delta\chi_l^2 = -\sum_{k,m}\frac{(k-m)^2}{l^2}\mathscr{E}[(p_k - p_{l-k+1})(p_m - p_{l-m+1})]. \tag{2.16}$$

The negative sign appears because $(p_k - p_{l-k+1})$ and $(p_m - p_{l-m+1})$ are in general anti-correlated in view of Eq. (2.14). We notice that the quantity $-\mathscr{E}[(p_k - p_{l-k+1})(p_m - p_{l-m+1})]$ in Eq. (2.16) is similar to the covariance $\mathrm{Cov}(p_k, p_m) \equiv \mathscr{E}\{[p_k - \mathscr{E}(p_k)][p_m - \mathscr{E}(p_m)]\}$, thus capturing the correlations between p_k and p_m as they appear within the window length l under time reversal. Hence, $\Delta\chi_l^2$ due to Eq. (2.16) may reveal non-trivial correlations between the elements of the time series Q_k.

Let us now assume that Q_k are long-range correlated, thus it may be justified to use the ansatz (see § 1.5.1.1):

$$-\mathscr{E}[(p_k - p_{l-k+1})(p_m - p_{l-m+1})] \propto \frac{(k-m)^{2\chi_H}}{l^2}, \tag{2.17}$$

where χ_H is a scaling exponent and we divided by l^2 because the probability p_k is expected to scale with $1/l$ in view of $\sum_{k=1}^{l} p_k = 1$. Substituting Eq. (2.17) into Eq. (2.16), we have

$$\Delta\chi_l^2 \propto l^{4+2\chi_H}/l^4 \tag{2.18}$$

so that

$$\Delta\chi_l \left(\equiv \sqrt{\Delta\chi_l^2}\right) \propto l^{\chi_H}. \tag{2.19}$$

Equation (2.19) reveals that the scaling exponent χ_H can be determined from the slope of the $\log \Delta\chi_l$ versus $\log l$ plot.

2.2.2.1 An example from fractional Brownian motion and fractional Gaussian noise time series

In order to examine the validity of the above result of Eq. (2.19) when the quantities Q_k come from fractional Brownian motion (fBm) or fractional Gaussian noise (fGn) (see § 1.5.1.1), we employ the following procedure. First, we generate fBm (or fGn) time series X_k (consisting of 2×10^4 points) for a given value of the self-similarity index H using the Mandelbrot–Weierstrass function [25, 44, 13] of Eq. (3.37) described in detailed later in § 3.4.3; see also Ref. [60]. Second, since Q_k should be positive, we normalize the resulting X_k time series to zero mean and unit standard deviation and then add to the normalized time series N_k a constant factor c to ensure the positivity of $Q_k = N_k + c$ (for the purpose of the present study we used $c = 10$). The resulting Q_k time series is then used for the calculation of the fluctuations of $\Delta\chi_l$ versus the scale l which are shown in Figs. 2.3(a) and 2.3(d) for fGn and fBm, respectively. The upper three panels of Fig. 2.3 correspond to fGn and the lower three to fBm. We observe that:

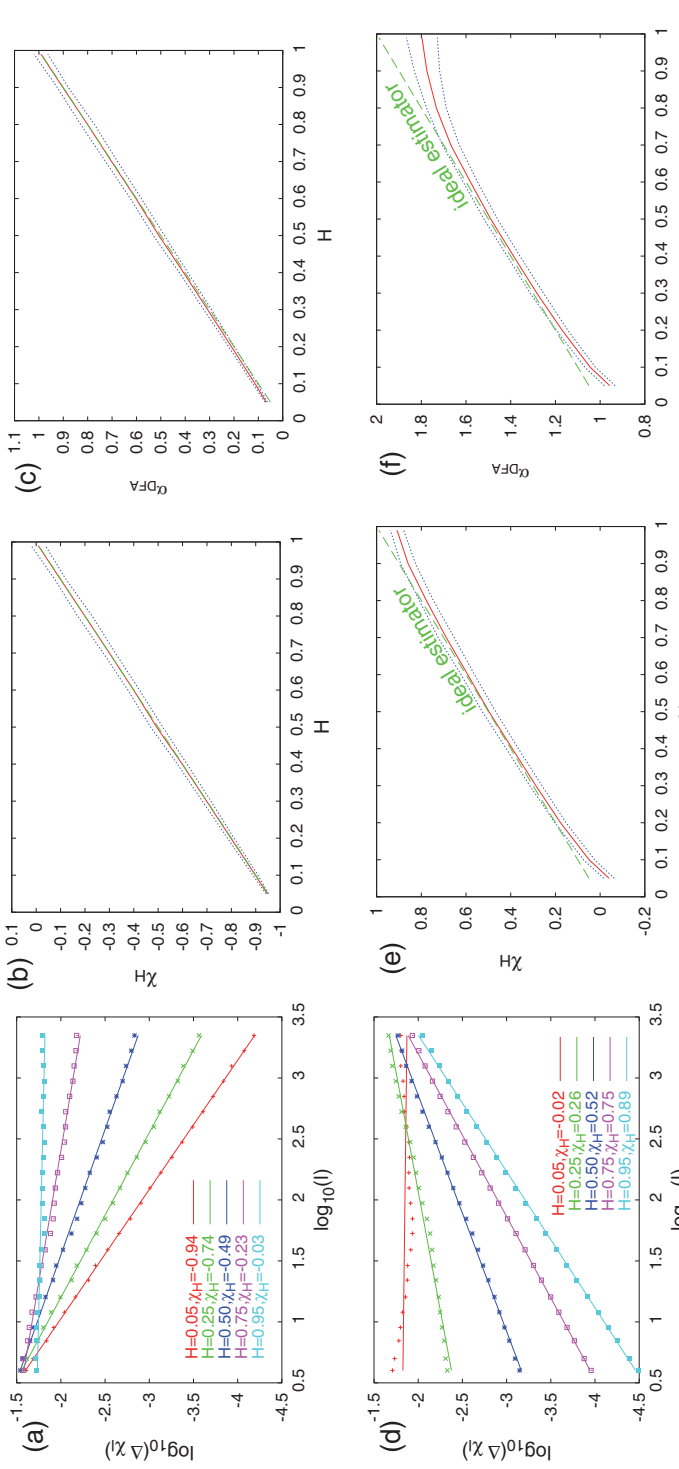

Fig. 2.3 Examples of log-log plot of the fluctuations $\Delta\chi_l$ of the natural time under time reversal versus the scale l for fGn (a) and fBm (d). (b) and (e) depict the values of the scaling exponent χ_H versus the self-similarity index H for fGn and fBm, respectively. For the sake of comparison, (c) and (f) are similar to (b) and (e), respectively, but for the DFA exponent α_{DFA}. The (blue) dotted curves show the $\pm\sigma$ deviation from the average value (obtained after 10^2 runs) depicted by the (red) solid curves. The (green) dashed straight lines correspond to the ideal behavior of each exponent and have been drawn as a guide to the eye. Reprinted with permission from Ref. [58]. Copyright (2008), American Institute of Physics.

For fGn we have the interconnection (see Fig. 2.3(b)) $\chi_H \approx H - 1$ corresponding to *descending* curves(see Fig. 2.3(a)).

For fBm the interconnection turns (see Fig. 2.3(e)) to $\chi_H \approx H$ corresponding to *ascending* curves (see Fig. 2.3(d)).

In order to judge the merits or demerits of the procedure proposed here for the determination of the scaling exponent, we compare Figs. 2.3(b) and 2.3(e) with Figs. 2.3(c) and 2.3(f), respectively, that have been obtained by DFA (§ 1.4.2). This comparison reveals that the results are more or less comparable for fGn, while for fBm the exponent χ_H deviates less from the behavior of an ideal estimator of the true scaling exponent (drawn in dashed green) compared to the exponent α_{DFA} obtained from the DFA method, especially for the largest H values.

2.3 Characteristic function. Mathematical background

Here, we recapitulate some useful properties related to the notion of the characteristic function in Probability Theory. These are given here without proofs, which can be found in Ref. [12]. For further studies see Ref. [7].

2.3.1 Definition of the characteristic function

Definition 2.1. Let X be a random variable with probability distribution F. The characteristic function of F (or of X) is the function φ defined for real ζ by

$$\varphi(\zeta) = \int_{-\infty}^{+\infty} \mathrm{e}^{i\zeta X} F\{\mathrm{d}X\} = u(\zeta) + iv(\zeta), \tag{2.20}$$

where $u(\zeta) = \Re[\varphi(\zeta)]$ and $v(\zeta) = \Im[\varphi(\zeta)]$.

For distributions F with a probability distribution function f

$$\varphi(\zeta) = \int_{-\infty}^{+\infty} \mathrm{e}^{i\zeta X} f(X)\, \mathrm{d}X. \tag{2.21}$$

According to Ref. [12], we make the following terminological note. In the accepted terminology of Fourier analysis φ is the *Fourier–Stieltjes transform of* F. Such transforms are defined for all bounded measures and the term "characteristic function" emphasizes that the measure has unit mass. (No other measures have characteristic functions.) On the other hand, integrals of the form (2.21) occur in many connections and one can say that Eq. (2.21) defines the *ordinary Fourier transform of* f. The characteristic function of F is the ordinary Fourier transform of the pdf f (when the latter exists), but the term Fourier transform applies also to other functions.

We now note that the function $\Phi(\omega)$, defined as

$$\Phi(\omega) = \frac{\sum_{k=1}^{N} Q_k \exp\left(i\omega\frac{k}{N}\right)}{\sum_{n=1}^{N} Q_n} = \sum_{k=1}^{N} p_k \exp\left(i\omega\frac{k}{N}\right), \tag{2.22}$$

is a characteristic function of p_k for *all* $\omega \in \mathscr{R}$.

2.3.2 Properties of the characteristic function

Definition 2.2. The moments m_n and the absolute moments M_n of X are given by

$$m_n = \int_{-\infty}^{+\infty} X^n F\{\mathrm{d}X\}, \tag{2.23}$$

and

$$M_n = \int_{-\infty}^{+\infty} |X|^n F\{\mathrm{d}X\}. \tag{2.24}$$

The following important theorem holds [12]:

Theorem 2.1. *If $M_n < \infty$, the n-th derivative of φ exists and is a continuous function given by*

$$\varphi^{(n)}(\zeta) = i^n \int_{-\infty}^{+\infty} \mathrm{e}^{i\zeta X} X^n F\{\mathrm{d}X\} \tag{2.25}$$

leading to

$$\varphi'(0) = im_1, \tag{2.26}$$
$$\varphi''(0) = -m_2, \tag{2.27}$$
$$\varphi'''(0) = -im_3, \text{ etc.} \tag{2.28}$$

It is important to note that the *converse* in Eq. (2.27) is also true: If $\varphi''(0)$ exists, then $m_2 < \infty$. For example, the function $\varphi_\alpha(\zeta) = \exp(-|\zeta|^\alpha)$ is *not* acceptable as a characteristic function *when* $\alpha > 2$, because the second moment of a distribution should be non-vanishing (note that this fact is important for understanding the applications of Lévy α-stable distributions in physics, e.g., see Refs. [27, 46, 47]).

Thus, the moments m_n of the distribution are calculated from the behavior of the characteristic function as $\zeta \to 0$.

There exists [12] another important theorem which describes the behavior of the characteristic function for large values of ζ: if F has a pdf f, then $\varphi(\zeta) \to 0$ as $\zeta \to \pm\infty$. If f has integrable derivatives $f', f'', \ldots, f^{(n)}$, then $|\varphi(\zeta)| = o(|\zeta|^{-n})$ as $|\zeta| \to \infty$.

2.4 The normalized power spectrum $\Pi(\omega)$ or $\Pi(\phi)$ and the variance κ_1 of natural time

For the purpose of natural time analysis, the following *continuous* function $\Phi(\omega)$, recall Eq. (2.22), was introduced [51, 52]:

$$\Phi(\omega) = \frac{\sum_{k=1}^{N} Q_k \exp\left(i\omega\frac{k}{N}\right)}{\sum_{n=1}^{N} Q_n} = \sum_{k=1}^{N} p_k \exp\left(i\omega\frac{k}{N}\right) = \sum_{k=1}^{N} p_k \, \mathrm{e}^{i\omega\chi_k} \tag{2.29}$$

where

$$\omega = 2\pi\phi, \tag{2.30}$$

ϕ standing for the frequency in natural time, termed *natural* frequency.

We then compute the normalized power spectrum $\Pi(\omega)$ as

$$\Pi(\omega) = |\Phi(\omega)|^2 = \left| \sum_{k=1}^{N} p_k \, \mathrm{e}^{i\omega\frac{k}{N}} \right|^2 \tag{2.31}$$

which does not change of course under time reversal. The function $\Phi(\omega)$ should not be confused with the *discrete* Fourier transform because ω is here a *continuous* variable.

Using Eq. (2.4), we have

$$\int_0^1 \mathrm{e}^{i\omega\chi} p(\chi)\, \mathrm{d}\chi = \sum_{k=1}^{N} \left[\int_0^1 p_k \delta(\chi - \chi_k)\, \mathrm{e}^{i\omega\chi}\, \mathrm{d}\chi \right] = \sum_{k=1}^{N} p_k \, \mathrm{e}^{i\omega\chi_k}, \tag{2.32}$$

thus $\Phi(\omega)$ can be written as

$$\Phi(\omega) = \int_0^1 \mathrm{e}^{i\omega\chi} p(\chi)\, \mathrm{d}\chi = \sum_{k=1}^{N} p_k \, \mathrm{e}^{i\omega\chi_k}. \tag{2.33}$$

If we regard $p(\chi)$ in Eq. (2.33) as the probability density function of χ, in analogy with probability theory, its Fourier transform $\Phi(\omega)$ may be regarded as the characteristic function of χ, representing the expectation value of $\mathrm{e}^{i\omega\chi}$ (see Eq. (2.21) in § 2.3.1).

By differentiations at the origin, i.e., as $\omega \to 0$, $\Phi(\omega)$ gives (see Theorem 2.1) the statistical properties of $p(\chi)$, such as the mean, variance etc. In view of Eq. (2.31), we now focus on the small ω values of $\Pi(\omega)$ by considering [51] its Taylor expansion, around $\omega = 0$,

$$\Pi(\omega) = 1 - \kappa_1\omega^2 + \kappa_2\omega^4 + \kappa_3\omega^6 + \kappa_4\omega^8 + \ldots \tag{2.34}$$

where

$$\kappa_1 = -\frac{1}{2}\frac{\mathrm{d}^2\Pi(\omega)}{\mathrm{d}\omega^2}\bigg|_{\omega=0}. \tag{2.35}$$

We now consider

$$\frac{\mathrm{d}^2\Pi(\omega)}{\mathrm{d}\omega^2} = \Phi^*(\omega)\frac{\mathrm{d}^2\Phi(\omega)}{\mathrm{d}\omega^2} + \Phi(\omega)\frac{\mathrm{d}^2\Phi^*(\omega)}{\mathrm{d}\omega^2} + 2\frac{\mathrm{d}\Phi(\omega)}{\mathrm{d}\omega}\frac{\mathrm{d}\Phi^*(\omega)}{\mathrm{d}\omega} \tag{2.36}$$

and taking into account Eq. (2.29) along with the fact that $\Phi(0) = 1$, we find:

$$\begin{aligned}\kappa_1 &= -\frac{1}{2}\left[-\sum_k p_k\chi_k^2 - \sum_k p_k\chi_k^2 + 2\left(\sum_k p_k\chi_k\right)^2\right] \\ &= \langle\chi^2\rangle - \langle\chi\rangle^2,\end{aligned} \tag{2.37}$$

where

$$\langle\chi^n\rangle = \sum_{k=1}^{N} p_k\chi_k^n \tag{2.38}$$

denote the moments of the natural time χ 'weighted' by p_k.

Thus, the quantity κ_1 corresponds to the variance of natural time:

$$\kappa_1 = \langle\chi^2\rangle - \langle\chi\rangle^2 = \sum_{k=1}^{N} p_k\left(\frac{k}{N}\right)^2 - \left(\sum_{k=1}^{N}\frac{k}{N}p_k\right)^2. \tag{2.39}$$

Since the normalized power spectrum $\Pi(\omega)$ does not change under time reversal, the same holds for κ_1.

The remaining terms of Eq. (2.34) can be shown [51] to be equal to

$$\kappa_2 = \frac{\langle\chi^2\rangle^2}{4} + \frac{\langle\chi^4\rangle}{12} - \frac{\langle\chi\rangle\langle\chi^3\rangle}{3} \tag{2.40}$$

$$\kappa_3 = \frac{\langle\chi^3\rangle^2}{36} + \frac{\langle\chi\rangle\langle\chi^5\rangle}{60} - \frac{\langle\chi^6\rangle}{360} - \frac{\langle\chi^2\rangle\langle\chi^4\rangle}{24} \tag{2.41}$$

$$\kappa_4 = \frac{\langle\chi^8\rangle}{20160} + \frac{\langle\chi^2\rangle\langle\chi^6\rangle}{720} + \frac{\langle\chi^4\rangle^2}{576} - \frac{\langle\chi^3\rangle\langle\chi^5\rangle}{360} - \frac{\langle\chi\rangle\langle\chi^7\rangle}{2520} \tag{2.42}$$

When considering the symmetric expansion of $p(\chi)$ in the region $[-1,1]$ which is obtained by selecting $p(0) \equiv \lim_{\chi\to 0} p(\chi)$ and $p(-\chi) \equiv p(\chi)$, we obtain that $p(\chi)$ can be expanded [51, 55] in a cosine Fourier series for $\chi \in (0,1]$:

$$p(\chi) = 1 + \sum_{n=1}^{\infty} \mathrm{p}_n \cos(n\pi\chi) \tag{2.43}$$

where

$$\mathrm{p}_n = 2\int_0^1 p(\chi)\cos(n\pi\chi)d\chi\,, \tag{2.44}$$

are the cosine Fourier series expansion coefficients. Equation (2.43) could give insight into what one should expect for the normalized power spectra $\Pi(\omega)$.

We recall that the lowest frequency included in this expansion, in addition to $\phi = 0$, is $\phi = 0.5$ corresponding to $\omega = \pi$.

Furthermore, $\Pi(\omega)$ for $\omega \ll \pi$, or $\phi \ll 0.5$, by virtue of the Taylor expansion (2.34) and Eqs. (2.39), (2.40), (2.41) and (2.42) resembles the properties of the characteristic function $\Phi(\omega)$ for $p(\chi)$ since its Taylor expansion coefficients are explicitly related to the moments of natural time χ. Of course, these moments do not appear in such a simple way as they appear in Theorem 2.1.

The detailed study of the quantity κ_1 shows that it exhibits (see Section 3.3) positivity, concavity, experimental stability and reveals that it has interesting physical properties; see Chapters 4 to 8.

By combining Eqs. (2.33), (2.35), (2.43) and (2.44), the following interrelation between κ_1 and the Fourier coefficients of $p(\chi)$ can be found [51]

$$\kappa_1 = \langle\chi^2\rangle - \langle\chi\rangle^2 = \frac{1}{12} + \frac{1}{2\pi^2}\sum_{n=1}^{\infty}\frac{\mathrm{p}_{2n}}{n^2} - \left[\frac{1}{2\pi^2}\sum_{k=0}^{\infty}\frac{\mathrm{p}_{2n+1}}{(n+1/2)^2}\right]^2. \tag{2.45}$$

We now calculate the limit for the variance κ_1 in the case of a *"uniform" distribution*, see § 2.1.3, for which $p(\chi) = 1$ and $\mathrm{p}_n = 0$. Thus, Eq. (2.45) leads to $\kappa_1 = 1/12$. This will be hereafter labeled κ_u, i.e.,

$$\kappa_u = \frac{1}{12} = 0.0833\ldots \tag{2.46}$$

The κ_1 value has been calculated in a variety of cases discussed in the present monograph. In particular, for SES activities it is theoretically obtained in § 2.4.2 and given in Table 4.6 for several experimental cases. The latter table also includes the κ_1 value for various "artificial" noises, and Table 4.4 the ionic current fluctuations in membrane channels. The κ_1 value for the case when the increments of the time series of Q_k are p.i.i.d. random variables of finite variance is calculated in § 2.5.3 and for power law distributed

(uncorrelated) energy bursts in § 2.5.4. For the case of fBm time series the κ_1 value will be discussed later in § 3.4.3 and for short-range correlated time series in § 3.4.5. As for dichotomous Markovian time series the κ_1 value will be treated in Chapter 4; see Fig. 4.22. Moreover, the κ_1 value for long-term seismicity will be discussed in Chapter 6, while for the seismicity that evolves after the initiation of SES activities and before the mainshock occurrence will be treated in Chapter 7 for several cases. Finally, for various dynamical models discussed in Chapter 8, the results for the κ_1 value when the critical point is approached are compiled in Table 8.1. Note also that the κ_1 values for a case when Q_k are *quasi-periodic* are depicted in Fig. 8.4.

The largest κ_1 value obtained either from experimental data or from theoretical models is 0.25. A theoretical explanation of this fact is given in § 3.3.2.1.

2.4.1 The normalized power spectrum for the "uniform" distribution

Using Eqs. (2.31) and (2.33), we obtain

$$\Pi(\omega) = \left| \int_0^1 \mathrm{e}^{i\omega\chi} p(\chi)\, \mathrm{d}\chi \right|^2 = \int_0^1 \int_0^1 p(\chi) p(\psi)\, \mathrm{e}^{i\omega(\chi-\psi)}\, \mathrm{d}\chi\, \mathrm{d}\psi \tag{2.47}$$

After the transformation of variables: $X = (\chi+\psi)/2$ and $\delta = (\chi-\psi)$, the double integral in Eq. (2.47) becomes

$$\Pi(\omega) = 2\int_0^1 \cos(\omega\delta) \int_{\frac{\delta}{2}}^{1-\frac{\delta}{2}} p\left(X-\frac{\delta}{2}\right) p\left(X+\frac{\delta}{2}\right)\, \mathrm{d}X\, \mathrm{d}\delta \tag{2.48}$$

Equation (2.48) can be also written as

$$\Pi(\omega) = 2\int_0^1 \cos(\omega\delta) G(\delta)\, \mathrm{d}\delta \tag{2.49}$$

with

$$G(\delta) = \int_{\frac{\delta}{2}}^{1-\frac{\delta}{2}} p\left(X-\frac{\delta}{2}\right) p\left(X+\frac{\delta}{2}\right)\, \mathrm{d}X \tag{2.50}$$

We can now estimate the normalized power spectrum $\Pi_u(\omega)$ for the *"uniform"* distribution. As already mentioned this is the case when Q_k are p.i.i.d. random variables. Thus, the pdf $p(\chi)$ becomes $p(\chi) = 1$ for all $\chi \in (0,1]$; Eq. (2.50) simply results in $G(\delta) = \int_{\frac{\delta}{2}}^{1-\frac{\delta}{2}} \mathrm{d}X = 1-\delta$ leading, see Eq. (2.49), to the normalized power spectrum

$$\Pi_u(\omega) = 2\int_0^1 (1-\delta)\cos(\omega\delta)\, \mathrm{d}\delta = \frac{\sin^2(\omega/2)}{(\omega/2)^2} \tag{2.51}$$

When expanding $\Pi_u(\omega)$ of Eq. (2.51) around $\omega \to 0$, we obtain

$$\Pi_u(\omega) \approx \left[1 - \frac{1}{3!}\left(\frac{\omega}{2}\right)^2\right]^2 \approx 1 - \frac{2}{3!}\left(\frac{\omega}{2}\right)^2 = 1 - \frac{1}{12}\omega^2 \tag{2.52}$$

When considering the expansion of Eq. (2.34), we observe that Eq. (2.52) results to $\kappa_1 = \kappa_u = 1/12$ in accordance with Eq. (2.46).

2.4.2 The normalized power spectrum of seismic electric signals

Here, we focus on the normalized power spectrum of SES activities which are emitted when criticality is approached [51, 52]. Thus, we rely on the physics behind their generation discussed in Section 1.6. We first consider the following two laboratory measurements. (i) Indentation experiments even in simple ionic crystals showed that transient electric signals are emitted, without the action of any external electric field, due to (formation and motion of) point and linear defects, e.g., see Ref. [62]. (ii) Independent measurements [37] revealed that, as the glass transition is approached, a polarization time series is emitted which probably arises from the reorientation process of electric dipoles; this process includes a large number of atoms (*cooperativity*). The feature of this polarization time series is strikingly similar [48] to the measured SES activities. This similarity is reminiscent of the pressure stimulated currents model [49] discussed in § 1.6.2, which suggests that upon a gradual variation of the pressure (stress) P on a solid, when approaching the *critical* pressure (stress) P_{cr}, transient electric signals are emitted arising from the (re)orientation of electric dipoles (formed due to defects). This emission occurs when the following condition is obeyed (which is just Eq. (1.48) of § 1.6.2):

$$\left.\frac{\mathrm{d}P}{\mathrm{d}t}\right|_T \frac{v^{m,b}}{kT} = -\frac{1}{\tau(P_{cr})}, \tag{2.53}$$

where $\left.\frac{\mathrm{d}P}{\mathrm{d}t}\right|_T$ is the pressure rate and $\tau(P_{cr})$ is the relaxation time of the dipoles at the critical pressure. It has been argued, see p. 404 of Ref. [49], that the values of the migration volume $v^{m,b}$ associated with SES generation should exceed the mean atomic volume by orders of magnitude, and this entails that the relevant (re)orientation process should involve the motion of a large number of "atoms" . Thus, the laboratory measurements fortify the suggestion [48] that the emission of the SES activities could be discussed in the frame of the theory of *dynamic phase transitions* (critical phenomena). The very stochastic nature of the relaxation process has been repeatedly discussed in the literature (see p. 350 of Ref. [19] and references therein; other suggestions have been reviewed in Ref. [31], while illuminating aspects have been forwarded in Ref. [66]). A stochastic analysis was based on the concept of clusters, the structural rearrangement of which develops in time [19]. According to this analysis the exponential relaxation of the polarization is arrested at a random time variable η_i and the instantaneous orientation reached at this instant is "frozen" at a

value $\exp(-\beta_i \eta_i)$ where $\beta_i = b =$ constant (see fig. 11.19 of Ref. [19]). Assuming that η_i itself follows an exponential distribution, with a time constant $\tau_0 \ll \tau(P_{cr})$, an almost constant current would be expected for as long as this unit "lives" (i.e., for a duration η_i).

As a result of *cooperativity*, the duration Q_k of a SES activity pulse is envisaged as the sum of n_k such identical units, thus $Q_k = \sum_{i=1}^{n_k} \eta_i$. Under this assumption, the duration Q_k of the k-th pulse in a SES activity follows the gamma distribution with a mean lifetime $n_k \tau_0$ and variance $n_k \tau_0^2$ (e.g., see lemma 8.1.6.5. of Ref. [30]), i.e., the average duration is given by:

$$\mathscr{E}(Q_k) = n_k \tau_0 \tag{2.54}$$

and its variance by:

$$\mathscr{E}(Q_k^2) - n_k^2 \tau_0^2 = n_k \tau_0^2. \tag{2.55}$$

As already mentioned (§ 1.6.2), the SES activity is emitted when the focal area enters into the critical regime. The approach of a system to a critical point can be characterized by a feature that events begin to be temporally correlated, which is equivalent to a persistent avalanching. The condition for the persistent avalanching can be expressed as

$$\mathscr{E}(Q_{k+1}) = Q_k \tag{2.56}$$

which means that the average Q_{k+1} value of the $k+1$-th event is maintained at the level already reached by the previous one. This is reminiscent of the aspect that the reorientation of a spin in the random-field Ising Hamiltonian, will cause on average just one more spin to flip at the critical point [23]. Since Q_{k+1} is assumed to be distributed according to the gamma distribution, we also have:

$$\begin{aligned} \mathscr{E}\left\{[Q_{k+1} - \mathscr{E}(Q_{k+1})]^2\right\} = \mathscr{E}(Q_{k+1})\tau_0 \Rightarrow \\ \mathscr{E}(Q_{k+1}^2) = Q_k \tau_0 + Q_k^2 \end{aligned} \tag{2.57}$$

We now turn to the evaluation of the normalized power spectrum $\Pi(\omega)$, see Eqs. (2.49) and Eq. (2.50), for the SES activities. We will first attempt to evaluate the average value $\tilde{G}(\delta)$

$$\tilde{G}(\delta) = \int_{\frac{\delta}{2}}^{1-\frac{\delta}{2}} \mathscr{E}\left[Q_{X-\frac{\delta}{2}} Q_{X+\frac{\delta}{2}}\right] \mathrm{d}X \tag{2.58}$$

as it results from all SES activities comprising N pulses. Note that $\tilde{G}(\delta)$ is similar to $G(\delta)$ of Eq. (2.50) apart from the fact that it does *not* involve the normalized pdfs $p(X - \frac{\delta}{2})p(X + \frac{\delta}{2})$. When for example $X - \frac{\delta}{2} = k/N$ and $X + \frac{\delta}{2} = l/N$, we have

$$\mathscr{E}[Q_{X-\frac{\delta}{2}} Q_{X+\frac{\delta}{2}}] = \mathscr{E}[Q_k Q_l] = \underbrace{\int \dots \int}_{N} Q_k Q_l \, \mathrm{d}\mathscr{P}_1 \, \mathrm{d}\mathscr{P}_2 \dots \mathrm{d}\mathscr{P}_k \dots \mathrm{d}\mathscr{P}_l \dots \mathrm{d}\mathscr{P}_N \tag{2.59}$$

where $\mathscr{P}_1, \mathscr{P}_2 \dots \mathscr{P}_N$ are the pdfs for the durations $Q_1, Q_2, \dots Q_N$, respectively. Using the normalization condition of the pdfs, we can eliminate the integrals over $\mathscr{P}_{l+1}$ to $\mathscr{P}_N$

$$\mathscr{E}[Q_k Q_l] = \underbrace{\int \dots \int}_{l} Q_k Q_l \, \mathrm{d}\mathscr{P}_1 \, \mathrm{d}\mathscr{P}_2 \dots \mathrm{d}\mathscr{P}_k \dots \mathrm{d}\mathscr{P}_l \tag{2.60}$$

and using Eq. (2.56) we can integrate over $\mathscr{P}_l$ down to $\mathscr{P}_k$

$$\mathscr{E}[Q_k Q_l] = \underbrace{\int \dots \int}_{k} Q_k^2 \, \mathrm{d}\mathscr{P}_1 \, \mathrm{d}\mathscr{P}_2 \dots \mathrm{d}\mathscr{P}_k \tag{2.61}$$

Performing now the integration over $\mathscr{P}_k$ by using the recursive relation of Eq. (2.57) for $k = k-1$, we obtain

$$\mathscr{E}[Q_k Q_l] = \underbrace{\int \dots \int}_{k-1} (Q_{k-1}\tau_0 + Q_{k-1}^2) \, \mathrm{d}\mathscr{P}_1 \, \mathrm{d}\mathscr{P}_2 \dots \mathrm{d}\mathscr{P}_{k-1} \tag{2.62}$$

whereas a second application of the recursive relations of Eqs. (2.56) and (2.57) into Eq. (2.62) results in

$$\mathscr{E}[Q_k Q_l] = \underbrace{\int \dots \int}_{k-2} (2Q_{k-2}\tau_0 + Q_{k-2}^2) \, \mathrm{d}\mathscr{P}_1 \, \mathrm{d}\mathscr{P}_2 \dots \mathrm{d}\mathscr{P}_{k-2}\,, \tag{2.63}$$

a third one to

$$\mathscr{E}[Q_k Q_l] = \underbrace{\int \dots \int}_{k-3} (3Q_{k-3}\tau_0 + Q_{k-3}^2) \, \mathrm{d}\mathscr{P}_1 \, \mathrm{d}\mathscr{P}_2 \dots \mathrm{d}\mathscr{P}_{k-3}\,, \tag{2.64}$$

and so on. Finally, we obtain

$$\mathscr{E}[Q_{X-\frac{\delta}{2}} Q_{X+\frac{\delta}{2}}] = \mathscr{E}[Q_k Q_l] = \int \left[(k-1)Q_1\tau_0 + Q_1^2\right] \, \mathrm{d}\mathscr{P}_1\,. \tag{2.65}$$

Restoring $k = (X - \frac{\delta}{2})N$ into Eq. (2.65), we obtain

$$\mathscr{E}[Q_{X-\frac{\delta}{2}} Q_{X+\frac{\delta}{2}}] = \alpha\left(X - \frac{\delta}{2}\right) + \beta, \tag{2.66}$$

where $\alpha = \int N\tau_0 Q_1 \, \mathrm{d}\mathscr{P}_1$ and $\beta = \int \left(Q_1^2 - \tau_0 Q_1\right) \mathrm{d}\mathscr{P}_1 = \left(\int Q_1 \, \mathrm{d}\mathscr{P}_1\right)^2$. Substituting Eq. (2.66) into Eq. (2.58), we obtain

$$\tilde{G}(\delta) = \int_{\frac{\delta}{2}}^{1-\frac{\delta}{2}} \left[\alpha\left(X - \frac{\delta}{2}\right) + \beta\right] \mathrm{d}X = \alpha\frac{(1-\delta)^2}{2} + \beta(1-\delta). \tag{2.67}$$

Equation (2.67) provides $\tilde{G}(\delta)$ for the SES activities comprising N pulses. We note the existence of two terms in the right-hand side of Eq. (2.67): The last term, which is simply

proportional to $(1-\delta)$, originates from the positivity of Q_k and is also present in the case of the "uniform" distribution, see Eq. (2.51). On the other hand, the first term $\frac{(1-\delta)^2}{2}$ comes from the *memory* of the critical process as reflected in Eq. (2.66), which states that the expectation $\mathscr{E}[Q_{X-\frac{\delta}{2}} Q_{X+\frac{\delta}{2}}]$ depends solely on $X-\frac{\delta}{2}$, i.e., the natural time elapsed since the initiation of the process.

In order to determine the normalized power spectrum for SES activities through a formula similar to Eq. (2.49), e.g.,

$$\Pi(\omega) = 2\int_0^1 \cos(\omega\delta)\mathscr{G}(\delta)\,\mathrm{d}\delta \tag{2.68}$$

we need also to average over all possible values of N to obtain an appropriate $\mathscr{G}(\delta)$. The quantity of $G(\delta)$ in Eq. (2.49), as well as $\mathscr{G}(\delta)$ in Eq. (2.68), is dimensionless since it results from the pdf $p(\chi)$ in Eq. (2.49). Equation (2.67) was obtained, however, without normalizing $Q_{X-\frac{\delta}{2}}$ and $Q_{X+\frac{\delta}{2}}$ by the appropriate factor $\left(\int Q_\chi\,\mathrm{d}\chi\right)^2$ because the inclusion of such a factor in the denominator would hinder the integration procedure followed. As a first approximation, we construct a dimensionless quantity from Eq. (2.67), thus for example we divide $\tilde{G}(\delta)$ by α:

$$\frac{\tilde{G}(\delta)}{\alpha} = \frac{(1-\delta)^2}{2} + \frac{\beta}{\alpha}(1-\delta). \tag{2.69}$$

The quantity $\mathscr{G}(\delta)$ is expected to be a weighted sum of the right-hand side of Eq. (2.69) for various values of N, thus it will be of the form

$$\mathscr{G}(\delta) \propto \frac{(1-\delta)^2}{2} + \overline{\left(\frac{\beta}{\alpha}\right)}(1-\delta), \tag{2.70}$$

where $\overline{\left(\frac{\beta}{\alpha}\right)}$ stands for the corresponding average – renormalized – value of the ratio

$$\frac{\beta}{\alpha} = \frac{\left(\int Q_1\,\mathrm{d}\mathscr{P}_1\right)^2}{\int N\tau_0 Q_1\,\mathrm{d}\mathscr{P}_1} = \frac{n_1}{N}. \tag{2.71}$$

Let us now impose (natural time) scale invariance which should hold for *criticality*. This means that the result should be independent of N. Hence, the time scale τ_0, so far arbitrary, should be such that the results obtained from Eq. (2.71) for various N lead to a value (labeled $\overline{\left(\frac{\beta}{\alpha}\right)}$ in Eq. (2.70)) *independent* of N. This is satisfied when $\tau_0 = \text{const.} \times Q_1/N$ as it is evident from Eq. (2.71). Since when a single SES pulse is emitted the only reasonable time scale to assume is that of the duration of the single pulse, we should impose $\tau_0 = Q_1/N$. Thus, we may write

$$\overline{\left(\frac{\beta}{\alpha}\right)} = \frac{\left(\int Q_1\,\mathrm{d}\mathscr{P}_1\right)^2}{\int Q_1^2\mathrm{d}\mathscr{P}_1}. \tag{2.72}$$

Assuming that at the initiation of the SES activity, only one unit is available, i.e, $n_1 = 1$, the duration Q_1 in Eq. (2.72) is exponentially distributed (see Eqs. (2.54) and (2.55)) leading to

$$\overline{\left(\frac{\beta}{\alpha}\right)} = \frac{1}{2}. \tag{2.73}$$

Equation (2.70) then reads

$$\mathscr{G}(\delta) \propto \frac{(1-\delta)^2}{2} + \frac{(1-\delta)}{2}. \tag{2.74}$$

Inserting Eq. (2.74) into Eq. (2.68), we obtain that for the SES activities (*critical dynamics*) the normalized power spectrum equals to [51]

$$\Pi(\omega) = \frac{18}{5\omega^2} - \frac{6\cos\omega}{5\omega^2} - \frac{12\sin\omega}{5\omega^3}. \tag{2.75}$$

Expanding Eq. (2.75) around $\omega = 0$ (see Eqs. (2.34) and (2.35)), we get

$$\Pi(\omega) \approx 1 - \kappa_1 \omega^2, \tag{2.76}$$

where

$$\kappa_1 = 0.070. \tag{2.77}$$

An inspection of Fig. 4.7 shows that for the region of natural frequencies $0 \leq \phi < 0.5$ (recall the shaded remark after Eq. (2.44)) the experimental results for the SES activities agree favorably with Eq. (2.75). In addition, for the SES activities observed to date, see Table 4.6, the validity of Eq. (2.77) has been confirmed.

An alternative derivation that $\kappa_1 \approx 0.070$ for SES activities, can be given on the basis of the Ising model if we also consider its qualitative similarity under certain conditions with the pressure-stimulated currents model (§ 1.6.2) for the SES generation, as will be explained in § 8.4.1.

Note that the relation $\kappa_1 = 0.070$, i.e., Eq. (2.77), emerges for several dynamical models approaching criticality which are compiled in Table 8.1.

2.5 Distinction of the origins of self-similarity

A large variety of natural systems exhibit irregular and complex behavior which at first looks erratic, but in fact possesses scale-invariant structure (e.g., see Refs. [34, 20]). As explained in § 1.5.1, a process $\{X(t)\}_{t\geq 0}$ is called self-similar [24] with index $H > 0$, if it has the property

$$X(\lambda t) \stackrel{d}{=} \lambda^H X(t) \qquad \forall \quad \lambda > 0. \tag{2.78}$$

Equation (2.78) means a "scale invariance" of the finite-dimensional distributions of $X(t)$, which does *not* imply, in stochastic processes, the same for the sample paths (e.g., see Ref. [65]). In this Section, following Ref. [59], we will explain how natural time enables the distinction of the two origins of self-similarity.

2.5.1 The two origins of self-similarity. Background

Examples of self-similar processes are Brownian, fractional Brownian (fBm), Lévy stable and fractional Lévy stable motion (fLsm). Lévy stable distributions (which are followed by many natural processes, e.g., see Refs. [46, 47]) differ greatly from the Gaussian ones because they have heavy tails and their variance is infinite (e.g., see Refs. [65, 38]).

An important point in analyzing data from natural systems that exhibit scale-invariant structure is the following. In several systems this nontrivial structure points to long-range *temporal* correlations; in other words, the self-similarity results from the process's memory *only* (e.g., the case of fBm discussed in § 1.5.1.1). Alternatively, the self-similarity may solely result from the process's increments' infinite variance, e.g., Lévy stable motion. (Note that in distributions that are applicable to a large variety of problems, extreme events have to be *truncated* for physical reasons, e.g., finite size effects – when there is no infinity [6] – and this is why we write hereafter "infinite".) In general, however, the self-similarity may result from both these origins (e.g., fLsm). It is the main aim of this Section to discuss how a distinction of the two origins of self-similarity (i.e., process's memory and process's increments' "infinite" variance) can be in principle achieved by employing natural time analysis.

Before proceeding, the following clarifications are necessary as far as the aforementioned two sources of self-similarity are concerned. Long-range temporal correlations, which are quoted above as a first origin of self-similarity, are an immediate consequence of Eq. (2.78) with $H > \frac{1}{2}$ defining a self-similar process. We stress, however, that long-range correlations do not automatically imply self-similarity of a process. Multifractal processes provide a large class of counter-examples (note that the natural time analysis of multiplicative cascades is discussed in § 6.2.5). The second origin of self-similarity comes from the statistical properties of the increments of the process. We emphasize, however, that the statistics of these increments does not automatically lead to nontrivial self-similarity of the process. Specifically, a process which is invariant under shuffling of the increments has independent increments and is characterized by the self-similarity index $\frac{1}{2}$.

2.5.2 The expectation value of κ_1 when a (natural) time window of length l is sliding through a time series

Here, we focus on the expectation value $\mathscr{E}(\kappa_1)$ of the variance (κ_1) of natural time when sliding a (time) window of length l through a time series of $Q_k > 0, k = 1,2,\ldots N$ (while in § 2.2.2 we calculated the fluctuations of the average value of the natural time itself under time reversal). In a window of length l starting at $k = k_0$, the quantities $p_j = Q_{k_0+j-1} / \sum_{m=1}^{l} Q_{k_0+m-1}$, $j = 1,2,\ldots,l$ are obtained, which satisfy the necessary conditions

$$p_j > 0, \tag{2.79}$$

$$\sum_{j=1}^{l} p_j = 1 \tag{2.80}$$

to be considered as point probabilities. We then define [51, 55] the moments of the natural time $\chi_j = j/l$ as $\langle \chi^q \rangle = \sum_{j=1}^{l} (j/l)^q p_j$ and hence

$$\kappa_1 = \sum_{j=1}^{l} \left(\frac{j}{l}\right)^2 p_j - \left[\sum_{j=1}^{l} \frac{j}{l} p_j\right]^2. \tag{2.81}$$

Note that κ_1 is a nonlinear functional of $\{p_j\}$. Let us consider the expectation value $\mu_j \equiv \mathscr{E}(p_j)$ of p_j. For the purpose of our calculation the relation between the variance of p_j, $\mathrm{Var}(p_j) \equiv \mathscr{E}[(p_j - \mu_j)^2]$, and the covariance of p_j and p_m, $\mathrm{Cov}(p_j, p_m) \equiv \mathscr{E}[(p_j - \mu_j)(p_m - \mu_m)]$, is important. In view of Eqs. (2.79) and (2.80), the quantities μ_j, $\mathrm{Var}(p_j)$ and $\mathrm{Cov}(p_j, p_m)$ are always finite independent of the presence of heavy tails in Q_k. Using the constraint of Eq. (2.80), leading to $p_j - \mu_j = \sum_{m \neq j} (\mu_m - p_m)$, we obtain

$$\mathrm{Var}(p_j) = -\sum_{m \neq j} \mathrm{Cov}(p_j, p_m). \tag{2.82}$$

We now turn to the evaluation of $\mathscr{E}(\kappa_1)$, and study its difference from the one that corresponds to the average time series $\mathscr{M} = \{\mu_k\}$ which is labeled $\kappa_{1,\mathscr{M}}$,

$$\kappa_{1,\mathscr{M}} = \sum_{j=1}^{l} \left(\frac{j}{l}\right)^2 \mu_j - \left[\sum_{j=1}^{l} \frac{j}{l} \mu_j\right]^2. \tag{2.83}$$

Hence,

$$\mathscr{E}(\kappa_1) - \kappa_{1,\mathscr{M}} = \mathscr{E}\left[\sum_{m=1}^{l} \frac{m^2}{l^2} (p_m - \mu_m) - \left(\sum_{m=1}^{l} \frac{m}{l} p_m\right)^2 + \left(\sum_{m=1}^{l} \frac{m}{l} \mu_m\right)^2\right]. \tag{2.84}$$

In view of the definition of μ_m, the first term in the right-hand side of Eq. (2.84) vanishes, whereas the latter two terms reduce to the variance of $\langle \chi \rangle$:

$$\mathscr{E}(\kappa_1) - \kappa_{1,\mathscr{M}} = -\mathscr{E}\left\{\left[\sum_{m=1}^{l} \frac{m}{l} (p_m - \mu_m)\right]^2\right\}. \tag{2.85}$$

Expanding this variance, we get

$$\kappa_{1,\mathscr{M}} - \mathscr{E}(\kappa_1) = \sum_{m=1}^{l} \frac{m^2}{l^2} \mathrm{Var}(p_m) + 2 \sum_{j=1}^{l-1} \sum_{m=j+1}^{l} \frac{jm}{l^2} \mathrm{Cov}(p_j, p_m). \tag{2.86}$$

which, upon using Eq. (2.82), leads to

$$\mathscr{E}(\kappa_1) - \kappa_{1,\mathscr{M}} = \sum_{j=1}^{l-1} \sum_{m=j+1}^{l} \frac{(j-m)^2}{l^2} \mathrm{Cov}(p_j, p_m) = \frac{1}{2} \sum_{j=1}^{l} \sum_{m=1}^{l} \frac{(j-m)^2}{l^2} \mathrm{Cov}(p_j, p_m)\,. \tag{2.87}$$

This relation turns to

$$\mathscr{E}(\kappa_1) = \kappa_{1,\mathscr{M}} + \sum_{\text{all pairs}} \frac{(j-m)^2}{l^2}\, \mathrm{Cov}(p_j, p_m)\,, \tag{2.88}$$

where $\sum_{\text{all pairs}} \equiv \sum_{j=1}^{l-1} \sum_{m=j+1}^{l}$ (compare Eq. (2.88) with Eq. (2.16) in which a term similar to the covariance $\mathrm{Cov}(p_j, p_m)$ has been discussed).

The case when Q_k do not exhibit temporal correlations: This is the case for example of randomly *shuffled* data. As the window is sliding through the whole time series, Q_k takes of course every position j within the window of length l. Then, Eq. (2.80) leads to

$$\mathscr{E}(p_j) = \frac{1}{l}\,, \tag{2.89}$$

and $\mathrm{Cov}(p_j, p_m)$ becomes independent of j and m, thus Eq. (2.82) becomes

$$\mathrm{Cov}(p_j, p_m) = -\frac{\mathrm{Var}(p)}{(l-1)}\,. \tag{2.90}$$

Since $\mathrm{Var}(p_j)$ is also independent of j, $\mathrm{Var}(p_j)$ was merely substituted by $\mathrm{Var}(p)$. Moreover, $\kappa_{1,\mathscr{M}}$ reduces to $\kappa_{1,c}$, where $\kappa_{1,c}$ corresponds to the constant time series $\mathscr{K} = \{x_k\}$: $x_k = 1/l, k = 1, 2, \ldots l$, which is given by

$$\kappa_{1,c} = \sum_{m=1}^{l} \frac{m^2}{l^3} - \left(\sum_{m=1}^{l} \frac{m}{l^2} \right)^2 = \kappa_u \left(1 - \frac{1}{l^2} \right)\,, \tag{2.91}$$

where $\kappa_u = 1/12 \approx 0.0833$. Turning now to Eq. (2.86) and by adding and subtracting $\frac{\mathrm{Var}(p)}{l-1} \sum \frac{m^2}{l^2}$, we obtain that:

For *shuffled* data

$$\mathscr{E}(\kappa_1) = \kappa_u \left(1 - \frac{1}{l^2} \right) - \kappa_u (l+1)\, \mathrm{Var}(p)\,. \tag{2.92}$$

In view of Eqs. (2.79) and (2.80), $\mathrm{Var}(p) < \mathscr{E}(p^2) < \mathscr{E}(p) = 1/l$, and thus the second term in Eq. (2.92) remains finite for $l \to \infty$.

The l-dependence of $\mathrm{Var}(p)$ when Q_k have a finite second moment is obtained from

$$\mathrm{Var}(p_k) = \frac{1}{l^2} \mathscr{E} \left[\left(\frac{l Q_k}{\sum_{n=1}^{l} Q_n} - 1 \right)^2 \right], \tag{2.93}$$

where the quantity $\mathscr{E}[(lQ_k/\sum_{n=1}^{l} Q_n - 1)^2]$ is *asymptotically* l-independent. The latter arises as follows: if $\mathscr{E}(Q_k) = \mu$ and $\mathrm{Var}(Q_k) = \sigma^2 (< \infty)$, as a result of the central limit theorem [12], we have $\mathscr{E}(\sum_{k=1}^{l} Q_k/l) = \mu$ and $\mathrm{Var}(\sum_{k=1}^{l} Q_k/l) = \sigma^2/l$. The latter two equations, for large enough l imply that $\mathscr{E}[(lQ_k/\sum_{n=1}^{l} Q_n - 1)^2] \approx \mathscr{E}[(Q_k/\mu - 1)^2] = \sigma^2/\mu^2$. Thus, Eq. (2.93) becomes (note that $\mathrm{Var}(p_k)$ is independent of k)

$$\mathrm{Var}(p) = \frac{\sigma^2}{l^2 \mu^2}. \tag{2.94}$$

For Q_k which do not exhibit time correlations, e.g., randomly shuffled data:

If Q_k do not exhibit heavy tails and have finite variance, $\mathrm{Var}(p)$ scales (Eq. (2.94)) as $1/l^2$, thus $\mathscr{E}(\kappa_1)$, as l increases in Eq. (2.92), converges to κ_u. The same holds for the most probable value $\kappa_{1,p}$ of κ_1.

Otherwise, the expectation value $\mathscr{E}(\kappa_1)$ differs from κ_u -pointing that $\kappa_{1,p}$ also differs from κ_u, i.e., $\kappa_{1,p} \neq \kappa_u$ – thus identifying the presence of heavy tails in the examined time series.

2.5.2.1 Comments on the expectation value of κ_1 for a given window length l

Let us now comment on the expectation value $\mathscr{E}(\kappa_1)$ of κ_1 when a (natural) time window of length l is sliding through a time series of $Q_k > 0$, which as mentioned (see Eq. (2.88)) is given by

$$\mathscr{E}(\kappa_1) = \kappa_{1,\mathscr{M}} + \sum_{\text{all pairs}} \frac{(j-m)^2}{l^2} \mathrm{Cov}(p_j, p_m), \tag{2.95}$$

Let us first discuss the case when Q_k are shuffled randomly. Equation (2.95) then turns to (see Eq. (2.92))

$$\mathscr{E}(\kappa_{1,shuf}) = \kappa_u \left(1 - \frac{1}{l^2}\right) - \kappa_u (l+1)\, \mathrm{Var}(p). \tag{2.96}$$

If Q_k do not exhibit heavy tails and have finite variance, Eq. (2.96) reveals (see the discussion above, § 2.5.2) that $\mathscr{E}(\kappa_{1,shuf})$ rapidly converges to κ_u. For example, this is the case of the SES activities [60] discussed in Chapter 4, e.g., see § 4.7.1. Otherwise, $\mathscr{E}(\kappa_{1,shuf})$ differs from κ_u, thus pointing to $\kappa_{1,p} \neq \kappa_u$. This is the case, for example, of the earthquakes discussed in Chapter 6.

Second, if Q_k do exhibit time correlations, the difference between the $\kappa_{1,p}$ for the original and the shuffled time series most likely originates from the difference of Eqs. (2.95) and (2.96), respectively. The extent to which the latter difference is nonzero accounts for the time correlations irrespective if Q_k exhibit heavy tails. For example, this is clearly the case of aftershocks and the case of earthquake catalogs in general (both of which exhibit heavy tails) discussed in detail in Section 6.3 (e.g., see Figs. 6.14 and 6.13, respectively).

The application of the above results to two important examples are given in the next two subsections.

2.5.3 The case when the increments of the time series of Q_k are positive i.i.d. random variables of finite variance

We first discuss the case when the increments of the time series of Q_k are p.i.i.d. random variables r_n of *finite* variance. In this case $Q_k = \sum_{n=1}^{k} r_n$, and hence Q_k is on average linearly related to k. Thus, it is expected that the continuous distribution $p(\chi)$, that corresponds to p_k see Eq. (2.4), is $p(\chi) = 2\chi$. Using

$$\kappa_1 = \int_0^1 p(\chi)\chi^2 \, \mathrm{d}\chi - \left(\int_0^1 p(\chi)\chi \, \mathrm{d}\chi \right)^2 , \tag{2.97}$$

a direct calculation leads to the value $\kappa_1 = \frac{1}{18} \approx 0.056$ which significantly differs from that $\kappa_u \approx 0.083$ of the "uniform" distribution (see Eq. (2.46)). In view of the fact that the increments have finite variance, the distribution of Q_k for a given N has also finite variance. Hence, as shown in the previous subsection, we expect that when Q_k are shuffled randomly the resulting κ_1 values should scatter around κ_u. A numerical example for exponentially distributed increments is shown in Fig. 2.4.

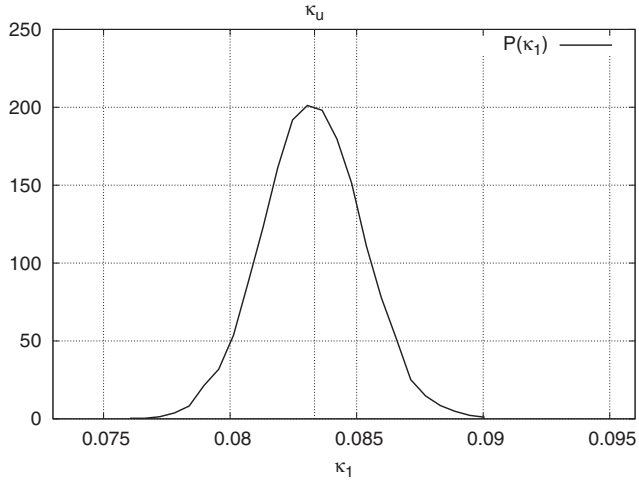

Fig. 2.4 The pdf of κ_1 that has been obtained by shuffling the Q_k *randomly* in the case of exponential increments, i.e., r_n are randomly drawn from an exponential distribution. Here, $N = 500$ and the original time series results in $\kappa_1 = 0.055$. See also Fig. 3.3.

2.5.4 The value of κ_1 when a (natural) time window is sliding through power law distributed energy bursts

We now study a case of self-similarity resulting from the process's increments' "infinite" variance. Here, we restrict ourselves to (slowly driven) systems that emit energy bursts obeying a power law distribution

$$P(E) \sim E^{-\gamma} \tag{2.98}$$

where γ is constant. In a large variety of such systems in diverse fields, an inspection of the experimental data reveals that the γ exponent lies in a narrow range $1.5 \leq \gamma \leq 2.1$ and mostly within even narrower bounds, i.e., $\gamma = 1.5$ to 1.8. To realize the diversity of the phenomena that exhibit the aforementioned property, we compile some indicative examples in Table 2.1, which are the following.

Table 2.1 Compilation of the experimental values of the power law exponent γ determined in different physical processes. Taken from Ref. [59].

Process / type of measurement	γ	References
Dislocation glide in hexagonal ice single crystals (acoustic emission)	1.6	[26]
Intermittent plastic flow in nickel microcrystals	1.6	[9]
Solar flares	1.5–2.1	[5, 32, 18, 29]
Microfractures before the breakup of wood (acoustic emission)	1.5	[14, 1]
Microfractures before the breakup of fiberglass (acoustic emission)	2.0	[14, 1]
Earthquakes	1.5–1.8	See Ref. [36] and references therein
Icequakes	$\approx$1.8	See p.212 of Ref. [64] and references therein

First, crystalline materials subjected to an external stress, display bursts of activity owing to the nucleation and motion of dislocations. These sudden local changes produce acoustic emission waves which reveal that a large number of dislocations move cooperatively in an intermittent fashion (e.g., see Ref. [22] and references therein). As a precise example, we include in Table 2.1 the results of acoustic emission experiments on stressed single crystals of ice under viscoelastic deformation (creep), which show that the probability distribution of energy bursts intensities obey a power law distribution with $\gamma = 1.6$ spanning many decades (see fig. 1 of Ref. [26]). Second, the same exponent is found [9] (i.e., $\gamma = 1.60 \pm 0.02$) in the analysis of intermittent plastic flow observations (i.e., measurements of discrete slip events for loadings above the elastic–plastic transition) on nickel microcrystals (see fig. 2 of Ref. [9]). Third, we consider the case of solar flares that represent impulsive energy releases in the solar corona (e.g. see Ref. [29] and references therein; see also Ref. [4] in which it is concluded that earthquakes and solar flares exhibit the same distributions of sizes, inter-occurrence times, and the same temporal clustering). This energy release is observed in various forms: thermal, soft and hard X-ray emissions, accelerated particles etc. The statistical analysis of these impulsive events show that the energy distribution exhibits, over several orders of magnitude, a power law with exponents

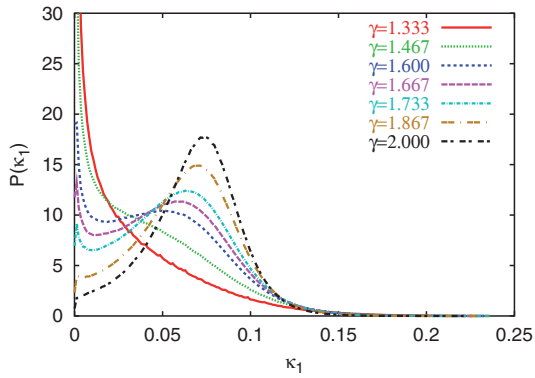

Fig. 2.5 The probability density function $P(\kappa_1)$ versus κ_1 for several values of γ. Taken from Ref. [59].

γ ranging from 1.5 to approximately 2.1 (depending on the experimental procedure and the geometrical assumptions adopted in the analysis). Other examples are: acoustic emission from microfractures before the breakup of heterogeneous materials (wood, fiberglass), icequakes and earthquakes.

The following procedure is now applied. We generate a large amount (500,000) of artificial data obeying Eq. (2.98) for a certain γ value with energy $E \geq 1$ and *randomly* shuffle them. This was repeated for various γ values by keeping the total number of events *constant* (which implies that when changing γ, the maximum energy involved in the calculation also changes). These *randomized* ("shuffled" [63, 56]) data are subsequently analyzed [61] in the natural time domain: the calculation of the variance κ_1 is made for an event taking time windows for $l = 6$ to 40 consecutive events (i.e., while in § 2.5.2 the value of l was kept constant, here l varies within certain limits and no κ_1 averaging is made). The choice of the precise value of the upper limit of l is not found decisive, since practically the same results are obtained even if the number of consecutive events was changed from 6–40 to 6–100. And second, this process was performed for all the events (for all the l

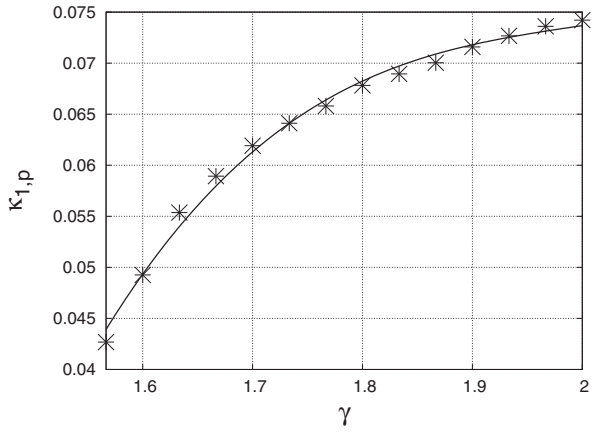

Fig. 2.6 The values of $\kappa_{1,p}$ as a function of γ for power law distributed data. The continuous line has been drawn as a guide to the eye. Note that $\kappa_{1,p} \approx 0.070$ for $\gamma \approx 1.87$, see also Fig. 2.5. Taken from Ref. [59].

values, e.g. between $l = 6$ to $l = 40$) by scanning the whole dataset. In Fig. 2.5, we plot the pdf $P(\kappa_1)$ versus κ_1 for several γ values. The most probable value $\kappa_{1,p}$ (for $\gamma =$ constant) is also plotted in Fig. 2.6 versus the corresponding γ value.

This curve interrelates κ_1 and γ for the shuffled data (thus an eventual process's memory is destroyed) and hence the plotted $\kappa_{1,p}$ values (which differ markedly from κ_u) correspond to the self-similarity resulting *solely* from the heavy-tailed distribution.

Note that the study of the origin of the self-similarity in real earthquake data will be elaborated in Chapter 6.

2.5.5 Conclusions

In summary, the origin of self-similarity may be distinguished as follows:

If self-similarity exclusively results from the process's memory, the κ_1 value should *change* to $\kappa_u = 1/12$ for the (randomly) shuffled data. This is the case of the SES activities, e.g. see § 4.7.1.

On the other hand, if the self-similarity results from process's increments' "infinite" variance *only*, the most probable value $\kappa_{1,p}$ should be the same (but differing from κ_u) for the original and the (randomly) shuffled data.

When both origins of self-similarity are present, the relative strength of the contribution of the one origin with respect to that of the other can be quantified on the basis of Eqs. (2.95) and (2.96), e.g., see § 6.3.2.

2.6 Origin of the optimality of the natural time representation

Here we address the problem [3] of optimality of the natural time representation of time series resulting from complex systems. For this purpose, we first study the structures of the time-frequency representations [7] of the signals by employing the Wigner function [68] to compare the natural time representation with the ones, either in conventional time or in other possible reparametrizations. We shall see that significant enhancement of the signal is observed in the time-frequency space if natural time is used, in marked contrast to other time domains. To quantify this localization property, we examine the generalized entropic measure proposed by Tsallis [45], which has been widely discussed in the studies of complex dynamical systems (see also Section 6.5).

In time series analysis, it is desired to reduce uncertainty and extract signal information as much as possible. Consequently, the most useful time domain should maximize the information measure, and hence minimize the entropy. We find that this can statistically be ascertained in natural time, by investigating a multitude of different time domains.

Consider a signal $\{x(t)\}$ represented in conventional time, t. The normalized time-frequency Wigner function associated with it is defined by

$$W(t,\omega) = A \int \mathrm{d}\tau \, \mathrm{e}^{-i\omega\tau} x(t-\tau/2)x(t+\tau/2), \tag{2.99}$$

where $A = [\pi \int \mathrm{d}t x^2(t)]^{-1}$ is the normalization constant and ω is the frequency. Numerically, it is necessary to discretize and make finite both time and frequency, and the integral has to be replaced by a sum. To make comparison of the natural time analysis with Eq. (2.99), it is convenient to rescale χ_k by $N\chi_k$, which is precisely the pulse number, $k \equiv t_k$. The quantity, Q_k , has a clear meaning for dichotomous time series (Fig. 2.1(a)), whereas for nondichotomous time series, threshold should be appropriately applied (e.g., the mean value plus half of the standard deviation) to transform it to a dichotomous one. The normalized Wigner function associated with Q_k is now given as follows:

$$W(k,\tilde{\omega}) = B \sum_{i=0}^{N-1} Q_{k-i} Q_{k+i} \cos[\tilde{\omega}(t_{k+i} - t_{k-i})], \tag{2.100}$$

where $B = [\pi \sum_{k=1}^{N} Q_k^2]^{-1}$ stands for the normalization constant and $\tilde{\omega}$ is the dimensionless "frequency". In the sum, Q_k with $k \leq 0$ and $k > N$ should be set equal to zero. Note that Eq. (2.100) is a discrete version of the continuous Wigner function in Eq. (2.99) and unlike the ordinary definition, the transformation in Eq. (2.100) is not orthogonal in general.

Figure 2.7 depicts the Wigner functions in the time-frequency spaces for the conventional time (a) and the natural time (b). Remarkably, significant enhancement of the signal is observed in the latter case, with the scale of enhancement being about 10 times. A localized structure emerges in natural time, in contrast to a moderate profile in the conventional time representation.

In the natural time domain, the time difference between two consecutive pulses (i.e., inter-occurrence time) is equally spaced and dimensionless, and is here taken to be unity: $t_{k+1} - t_k = 1$. However, for the sake of comparison, we will later consider various time domains in which the occurrence time $t_k = Nu_k$ in Eq. (2.100) is made random. The conventional time representation is characterized by a constant time increment Δt (e.g., 1 sec), and the occurrence of the i-th event is at $t_i = i\Delta t$. To generate the random time domains artificially, we consider uniformly distributed u_k so that the average inter-occurrence time is again unity. Performing Monte-Carlo simulation, we have constructed more than 1,000 different time domains and integrated over ω ($\tilde{\omega}$) over 0 to π [rad/sec] ([rad]), which can cover the regimes of interest (recall that when $t_k = k$, $W(k,\omega+\pi) = W(k,\omega)$).

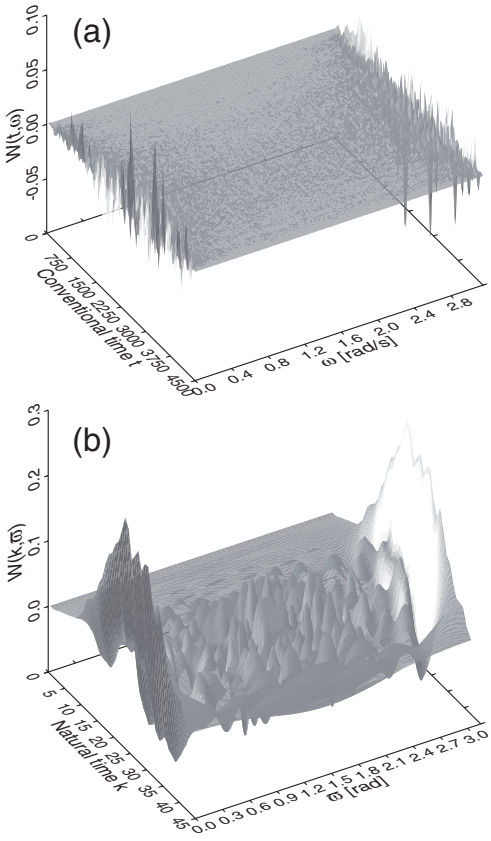

Fig. 2.7 The plots of the Wigner functions of the SES activity A of Fig. 2.8 given below in (a) the conventional time domain and (b) the natural time domain. Significant enhancement of the signal is recognized in the natural time domain at both edges but mainly in the localized structures in the intermediate region. Note that, instead of χ_k, $N\chi_k = k$ is used (see the text). ω has the unit [rad/sec], whereas has $\tilde{\omega}$ has [rad]. Taken from Ref. [3].

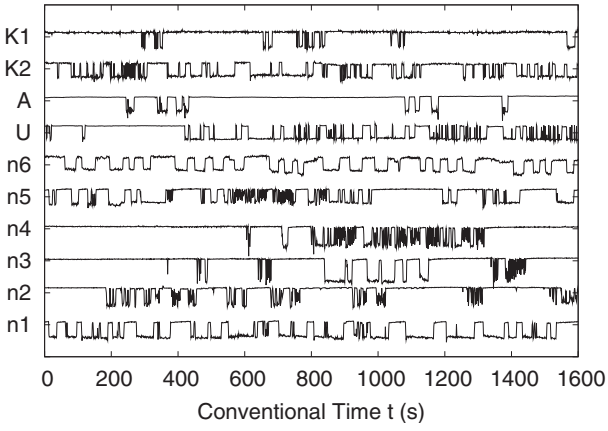

Fig. 2.8 Excerpts of 4 SES activities, labeled K1, K2, A, U and 6 "artificial" noises, labeled n1–n6, in normalized units, see the caption of Fig. 4.2. Taken from Ref. [3].

To quantify the degrees of disorder in the time-frequency spaces with various time domains, we employ as mentioned the Tsallis entropy [45] defined by

$$S_q = \frac{1}{1-q}\left(\int \mathrm{d}\mu W^q - 1\right), \tag{2.101}$$

where $\int \mathrm{d}\mu$ is the collective notation for integral and sum over the time-frequency space and q is the positive entropic index. In the limit $q \to 1$, this quantity tends to the form of the Boltzmann–Gibbs–Shannon entropy $S = -\int \mathrm{d}\mu W \ \ln W$. This limit cannot however be taken, since the Wigner function is a pseudo-distribution and takes negative values, in general. The quantity S_q is, however, well defined if q is even. Thus, we propose to use the value

$$q = 2, \tag{2.102}$$

which, by considering Eqs. (2.100) and (2.101), results in:

$$S_2 = 1 - \frac{1}{2\pi} \times \left\{ \frac{\sum_{k=1}^{N}\sum_{l=0}^{N-1}\sum_{l'=0}^{N-1} Q_{k-l}Q_{k+l}Q_{k-l'}Q_{k+l'} \frac{\sin[\pi(t_{k+l}-t_{k-l}+t_{k+l'}-t_{k-l'})]}{\pi(t_{k+l}-t_{k-l}+t_{k+l'}-t_{k-l'})}}{\left[\sum_{k=1}^{N}\left(Q_k^2 + \sum_{l=1}^{N-1} Q_{k-l}Q_{k+l}\frac{\sin[\pi(t_{k+l}-t_{k-l})]}{\pi(t_{k+l}-t_{k-l})}\right)\right]^2} + \right.$$
$$\left. \frac{\sum_{k=1}^{N}\sum_{l=0}^{N-1}\sum_{l'=0}^{N-1} Q_{k-l}Q_{k+l}Q_{k-l'}Q_{k+l'}\left(\delta_{l+l',0} + \delta_{l,l'} + \frac{\sin[\pi(t_{k+l}-t_{k-l}-t_{k+l'}+t_{k-l'})]}{\pi(t_{k+l}-t_{k-l}-t_{k+l'}+t_{k-l'})}\right)}{\left[\sum_{k=1}^{N}\left(Q_k^2 + \sum_{l=1}^{N-1} Q_{k-l}Q_{k+l}\frac{\sin[\pi(t_{k+l}-t_{k-l})]}{\pi(t_{k+l}-t_{k-l})}\right)\right]^2} \right\} \tag{2.103}$$

Table 2.2 The values of $\mathrm{Prob}(S_2 < S_2^{nat})$ together with the number of pulses N for the electric signals of Fig. 2.8 with $N > 50$. The estimation error is at the most 1.6%.

Signal	N	$\mathrm{Prob}(S_2 < S_2^{nat})(\%)$
K1	312	3.7
K2	141	6.9
U	80	8.1
n1	216	5.7
n2	1080	<0.1
n3	259	2.7
n4	396	1.6
n5	432	2.8

To examine how the natural time representation is superior to other ones, in Ref. [3] we made comparison of the values of S_2 for 10 different time series [54] of electric signals (see Fig. 2.8, whereas Fig. 4.9 depicts their natural time representation): 4 SES activities and 6 "artificial" noises. The results of 8 (out of the 10) signals comprising more than 50 pulses are compiled in Table 2.2 in which we give the values of $\mathrm{Prob}(S_2 < S_2^{nat})$, i.e.,

the probability that S_2 calculated for a time domain different than the natural time domain to be smaller than the value S_2^{nat} calculated for natural time (note that this value comes from Eq. (2.103) and should not be confused with the entropy S in natural time defined by Eq. (3.1), see Chapter 3). This probability Prob$(S_2 < S_2^{nat})$ was estimated as follows. For each time domain produced by Monte–Carlo the corresponding S_2 value was calculated through Eq. (2.103) and compared to S_2^{nat}. For signals with a reasonable number of pulses, e.g., larger than 50, Table 2.2 reveals that the quantity S_2^{nat}, in fact, tends to be minimum compared to those of other representations attempted. In addition, it is mentioned that S_2^{nat} is also appreciably smaller than S_2 in conventional time (see Fig. 2.7).

In conclusion, we investigated if natural time yields an optimal representation for enhancing the signals in the time-frequency space by employing the Wigner function and measuring its localization property by means of the Tsallis entropy. For this purpose, we compared the values of the entropy for various time series (being either SES activities or "artificial" noises) represented in a multitude of different time domains. We find that the entropy is highly likely to be minimum for natural time, implying the least uncertainty in the time-frequency space. This explains why dynamical evolution of diverse systems can be better described in natural time.

2.7 Is time continuous?

Natural time χ, from its definition, is *not continuous* and takes values which are *rational* numbers in the range (0,1]. (In these numbers, as the complex system evolves, the numerators are just the natural numbers (except 0), which denote the *order* of appearance of the consecutive events.) Hence, one of the fundamental differences between (conventional) time and natural time refers to the fact that the former is based on the idea of *continuum*, while the latter is *not*. Following Ref. [50], here we aim at raising some consequences of this difference, and in particular those that stem from the *set theory* developed by Cantor, having in mind the following *crucial* remark made by Schrödinger (see pp. 62–63 of Ref. [40]):

"We are familiar with the idea of the *continuum*, or we believe ourselves to be. We are *not* familiar with the enormous difficulty this concept presents to the mind, unless we have studied very modern mathematics (Dirichlet, Dedekind,Cantor)."

2.7.1 Differences between natural time and conventional time on the basis of set theory

We clarify in advance that we do not tackle here the case (since it is inapplicable to our universe [16]) raised by Gödel in 1949 who discovered [15] unexpected solutions to the equations of general relativity corresponding to universes in which *no universal temporal ordering is possible* (see also Refs. [8, 71] and references therein). This solution acquires

its simplest form (see p.86 in Ref. [39]) "with *two* of the coordinate-line-elements time-like (the other two space-like)". Interestingly, Schrödinger in an early version of Ref. [39], which was published almost simultaneously with Gödel's work, had also emphasized that "there is no necessity for just three of the four line-elements being space-like, one time-like ...".

We now recapitulate some points of the Cantor set theory that are relevant to our present discussion.

A *transfinite number or transfinite cardinal* is the cardinality of some *infinite* set, where the term *cardinality* of a set stands for the number of members it contains, e.g., see Ref. [43].

The set of natural numbers is labeled by $\mathscr{N}$, while the number of natural numbers is designated by $\aleph_0$, i.e., $\aleph_0 = |\mathscr{N}|$ (note that the cardinality of a set S is labeled $|S|$). In this transfinite number, the zero subscript is justified by the fact that, as proved by Cantor, no infinite set has a smaller cardinality than the set of natural numbers.

It can be shown that the set of rational numbers designated by $\mathscr{Q}$ has the same cardinality as the set of natural numbers, or $|\mathscr{N}| = |\mathscr{Q}|$ (e.g., Theorem 2 in Ref. [43]). In other words, the rationals are *exactly* as numerous as the naturals.

Note that a set is *countable iff* its cardinality is either finite or equal to $\aleph_0$ and in particular is termed *denumerable iff* its cardinality is exactly $\aleph_0$ (note that as usually, for "if and only if" we write simply "*iff*"). A set is *uncountable iff* its cardinality is greater than $\aleph_0$; see also below.

Hence, natural time takes values (which, as mentioned, are rational numbers) that form in general a *countable* set; this becomes a *denumerable* set in the limit of infinitely large number of events (see § 2.7.2).

Further, since in natural time analysis we consider the pairs (χ_k, Q_k), the values of the quantity Q_k *should* form a set with cardinality smaller than (or equal to) $\aleph_0$. In other words, the values of the energy also form a *countable* set, which reflects of course that the energy is *not continuous*, thus the *quantization of energy* seems to emerge.

The fact that $|\mathscr{N}| = |\mathscr{Q}|$ is an astounding result in view of the following. The rational numbers are *dense* in the real numbers, which means that between any two rational numbers on the real number line we can find *infinitely more* rational numbers. In other words, although the set of rational numbers seems to contain infinities within infinities, there are just as many natural numbers as there are rational numbers. This reflects the following point.

Let us assume that we follow the evolution of a system with some (experimental) accuracy, in which, as mentioned, in the limit of infinitely large number of events the cardinality

of the set of the values of natural time is $\aleph_0$. Let us assume that we now repeat the measurement with more sensitive instrumentation, i.e., counting events above an appreciably smaller energy threshold (which should be constrained by the uncertainty principle, but a further discussion on this point lies beyond the scope of the present monograph, as already mentioned in § 2.1.1); hence between two consecutive events of the former measurement a considerable number of appreciably smaller events may be monitored. The corresponding cardinality, in contrast to our intuition, is again $\aleph_0$. In other words, when considering the limit of infinitely large number of consecutive events, the natural time takes values that form a *denumerable* set and this remains so even upon increasing the accuracy (and hence lowering the uncertainty) of our measurement. The inverse, i.e., when the instrumentation becomes less sensitive, may correspond to a "coarse graining" procedure.

We now turn to the aspects of Cantor set theory related to the real numbers, which as mentioned are associated with the conventional time. It is shown that the number of points on a finite line segment is the same as the number of points on an infinite line (e.g., Theorem 13 in Ref. [43]). Considering the definition: the number of real numbers is the same as the number of points on an infinite line (or in the jargon, the *numerical continuum* has the same cardinality as the *linear continuum*), let "c" designate the cardinality of the continuum – or equivalently the cardinality of the set of real numbers. (Hence $c = |\mathscr{R}|$ by definition.) It is proven (e.g., Theorem 16 in Ref. [43]) that the set of real numbers is uncountable, or $|\mathscr{R}| > \aleph_0$. (Equivalently, this theorem asserts that $c > \aleph_0$.)

Hence, the values of conventional time form an *uncountable* set, in contrast to that of natural time which in general as mentioned is countable.

In order to further inspect this fundamental difference, we resort to the continuum hypothesis (CH) which was formulated (but not proved) by Cantor.

Continuum hypothesis, after Euclid's parallel postulate, was the first major conjecture to be proved *undecidable* by standard mathematics [43].

We first clarify that the power set ${}^*S$ of a set S, which is the set of all subsets of S, has a cardinality $|{}^*S| = 2^{|S|}$ when S is finite. According to Cantor's Theorem the cardinality of the power set of an *arbitrary* set has a greater cardinality than the original arbitrary set, i.e., $|{}^*S| > |S|$ (e.g., Theorem 4 in Ref. [43]). This theorem is trivial for finite sets, but fundamental for infinite sets. Hence, for any infinite cardinality, there is a larger infinite cardinality, namely, the cardinality of its power set.

The continuum hypothesis asserts that there is *no* cardinal number α such that $\aleph_0 < \alpha < c$.

Then it follows that the next largest transfinite cardinal after $\aleph_0$ (labeled $\aleph_1$) is c, thus $c = \aleph_1$. Since Cantor proved (e.g., Theorem 17 in Ref. [43]) that $\aleph_1 = 2^{\aleph_0}$, CH leads to: $c = 2^{\aleph_0}$ (thus, this is the number of points on an infinite line).

Hence, if we assume CH, the cardinality of the set of the values of natural time – in the limit of infinitely large number of events – corresponds to $\aleph_0$, while that of the conventional time is $2^{\aleph_0}$.

The values of the former, as mentioned, are rational numbers, while almost all the values of the latter are *irrational*, because, since $2^{\aleph_0} \gg \aleph_0$, almost all reals are irrational numbers. (On the other hand, without assuming CH we have essentially *no idea* which transfinite number corresponds to c, and we would know the cardinality of the naturals, integers, and rationals, but *not* the cardinality of the reals, e.g., see Ref. [43].) As for the values of Q_k, they are *not* necessarily rational, because in general when taking $\aleph_0$ (at the most) out of $2^{\aleph_0}$ values they may all be irrational.

Hence, in the limit of infinitely large number of events, even upon gradually improving the accuracy of our measurements, both sets $\{\chi_k\}$ and $\{Q_k\}$ remain denumerable, the former consisting of rational numbers only.

2.7.2 Proof of the cardinality of the set of the values of natural time

We now indicate how in the limit of infinitely large number of events we conclude that the cardinality of the set of the values of natural time equals to $\aleph_0$. Let us tabulate the values of natural time upon the occurrence of each event:

after the first event	1					
after the second event	$\frac{1}{2}$	$\frac{2}{2}$				
after the third event	$\frac{1}{3}$	$\frac{2}{3}$	$\frac{3}{3}$			
after the fourth event	$\frac{1}{4}$	$\frac{2}{4}$	$\frac{3}{4}$	$\frac{4}{4}$		
...						
after the Nth event	$\frac{1}{N}$	$\frac{2}{N}$	$\frac{3}{N}$	$\frac{4}{N}$	...	$\frac{N}{N}$

This indicates that the cardinality of the set of the values of natural time $|\{\chi_k\}|$ should be greater than (or equal to) N(number of entries in the first column) and smaller than (or equal to) N^2 (number of entries in the square $N \times N$ matrix), i.e.,

$$N \leq |\{\chi_k\}| \leq N^2. \tag{2.104}$$

Thus, for $N \to \infty$ we have $\aleph_0 \leq |\{\chi_k\}| \leq \aleph_0^2$ and since $\aleph_0^2 = \aleph_0$ (see Theorem 22 of Ref. [43]), we find that $|\{\chi_k\}| = \aleph_0$.

2.7.3 Is natural time compatible with Schrödinger's point of view?

Schrödinger, in order to point out "the intricacy of the continuum", used the following example (see pp. 138–143 of Ref. [41]): Let us consider the interval [0,1], you first take

away the whole middle third including its left border point, thus the points from 1/3 to 2/3 (but you leave 2/3). Of the remaining two-thirds you again take away "the middle thirds", including their left border points, but leaving their right border points. With the remaining "four ninths" you proceed in the same way and so on. The cardinality of the set that remains *ad infinitum* is no less than that of [0,1] because it can be shown [41] that there is a one-to-one correspondence between their elements. Moreover, since it is a subset of [0,1], its cardinality is also no greater, so it must in fact be equal. In particular, Schrödinger concludes [41] as follows: "The remarkable fact about our remaining set is that, although it covers no measurable interval, yet it still has the vast extension of any continuous range. This astonishing combination of properties is, in mathematical language, expressed by saying that our set has still the 'potency' of the continuum, although it is 'of measure zero'." In other words, the cardinality of the aforementioned remaining set considered by Schrödinger exceeds drastically that of the set of the values of natural time.

Let us now comment on the common view that (conventional) time is continuous, keeping in the frame that, as pointed out by Schrödinger (p. 145 of Ref. [42]) "our sense perceptions constitute our sole knowledge about things". In short, it seems that the continuity of time does not stem from *any* fundamental principle, but probably originates from the following demand on continuity discussed by Schrödinger (see p. 130 of [41]):

"From our experiences on a large scale ... physicists had distilled the one clear-cut demand that a truly clear and complete description of any physical happening has to fulfill: it ought to inform you precisely of what happens at any point in space at any moment of time .... We may call this demand the *postulate of continuity of the description*."

Schrödinger, however, subsequently commented on this demand as follows (see p. 131 of Ref. [41]): "It is this postulate of continuity that appears to be unfulfillable!..." and furthermore added: "We *must not admit the possibility of continuous observation*." Considering these important remarks, we may say that the concept of natural time is not inconsistent with Schrödinger's point of view.

2.7.4 Conclusions

Conventional time is currently assumed continuous, but this does not necessarily result from *any* fundamental principle. Its values form an uncountable set, almost all of which may be *irrational* numbers. On the other hand, natural time is not continuous, and its values form a countable set consisting of rational numbers only; further, the values of the energy also form a countable set but they are not necessarily rational. In the limit of infinitely large number of events, the cardinality of the set of the values of natural time is $\aleph_0$ (irrespective of whether we increase the accuracy of the measurement), thus being drastically smaller than that of conventional time, which equals to $2^{\aleph_0}$ if we accept the validity of the continuum hypothesis.

References

1. A. Guarino, S. Ciliberto, A. Garcimartín, M. Zei, R. Scorretti: Failure time and critical behaviour of fracture precursors in heterogeneous materials. Eur. Phys. J. B **26**(2), 141–151 (2002)
2. Concluding the 23^{rd} Solvey Conference (Dec. 2005), David Gross, compared the state of Physics today to that during the first Solvay conference in 1911 and said: "They were missing something absolutely fundamental" he said. "We are missing perhaps something as profound as they were back then", see New Scientist, December 10, pp.6,7 (2005).
3. Abe, S., Sarlis, N.V., Skordas, E.S., Tanaka, H.K., Varotsos, P.A.: Origin of the usefulness of the natural-time representation of complex time series. Phys. Rev. Lett. **94**, 170601 (2005)
4. de Arcangelis, L., Godano, C., Lippiello, E., Nicodemi, M.: Universality in solar flare and earthquake occurrence. Phys. Rev. Lett. **96**, 051102 (2006)
5. Aschwanden, M.J., Nightingale, R.W., Tarbell, T.D., Wolfson, C.J.: Time variability of the "quiet" Sun observed with TRACE, II. Physical parameters, Temperature Evolution, and Energetics of Extreme-Ultraviolet-Nanoflares. Astrophys. J. **535**, 1047–1065 (2000)
6. Ausloos, M., Lambiotte, R.: Brownian particle having a fluctuating mass. Phys. Rev. E **73**, 011105 (2006)
7. Cohen, L.: Time-Frequency Analysis. Theory and Applications. Prentice-Hall, Upper Saddle River, NJ (1994)
8. Davis, M.: Gödel's universe. Nature **435**, 19–20 (2005)
9. Dimiduk, D.M., Woodward, C., LeSar, R., Uchic, M.D.: Scale-free intermittent flow in crystal plasticity. Science **312**, 1188–1190 (2006)
10. Einstein, A.: *Ideas and Opinions* (Crown Publishers, 1954; new edition by Souvenir Press, 2005); see also p. 54 in A. Gefter in New Scientist, 10 December, 2005
11. Einstein, A.: A brief outline of the developement of the theory of relativity. Nature **106**, 782–784 (1921)
12. Feller, W.: An Introduction to Probability Theory and Its Applications, Vol. II. Wiley, New York (1971)
13. Frame, M., Mandelbrot, B., Neger, N.: Fractal Geometry, Yale University, available from http://classes.yale.edu/fractals/, see http://classes.yale.edu/Fractals/RandFrac/fBm/fBm4.html
14. Garcimartín, A., Guarino, A., Bellon, L., Ciliberto, S.: Statistical properties of fracture precursors. Phys. Rev. Lett. **79**, 3202–3205 (1997)
15. Gödel, K.: An example of a new type of cosmological solutions of Einstein's field equations of gravitation. Rev. Mod. Phys. **21**, 447–450 (1949)
16. Hentschel, K.: Review of: A world without time: The forgotten legacy of Gödel and Einstein. Physics Today **58(12)**, 60–61 (2005)
17. Hooft, G.T.: In *Does God play dice*? Physics World, December 2005, (http://physicsweb.org/articles/world)
18. Hughes, D., Paczuski, M., Dendy, R.O., Helander, P., McClements, K.G.: Solar flares as cascades of reconnecting magnetic loops. Phys. Rev. Lett. **90**, 131101 (2003)
19. Jonscher, A.K.: Universal Relaxation Law. Chelsea Dielectric Press, London (1996)
20. Kalisky, T., Ashkenazy, Y., Havlin, S.: Volatility of linear and nonlinear time series. Phys. Rev. E **72**, 011913 (2005)
21. Kanamori, H.: Quantification of earthquakes. Nature **271**, 411–414 (1978)
22. Koslowski, M., LeSar, R., Thomson, R.: Avalanches and scaling in plastic deformation. Phys. Rev. Lett. **93**, 125502 (2004)
23. Kuntz, M.C., Sethna, J.P.: Noise in disordered systems: The power spectrum and dynamic exponents in avalanche modelss. Phys. Rev. B **62**, 011699 (2000)
24. Lamperti, J.W.: Semi-stable stochastic processes. Trans. Am. Math. Soc. **104**, 62–78 (1962)
25. Mandelbrot, B.B., Wallis, J.R.: Some long-run properties of geophysical records. Water Resources Research **5**, 321–340 (1969)
26. Miguel, M.C., Vespignani, A., Zapperi, S., Weiss, J., Grasso, J.R.: Intermittent dislocation flow in viscoplastic deformation. Nature **410**, 667–671 (2001)

27. Montroll, E.W., Bendler, J.T.: On Lévy (or stable) distributions and the Williams-Watts model of dielectric relaxation. J. Stat. Phys. **34**, 129–162 (1984)
28. von Neumann, J.: Mathematical Foundations of Quantum Mechanics. Princeton University Press, Princeton N.J. (1955)
29. Nigro, G., Malara, F., Carbone, V., Veltri, P.: Nanoflares and mhd turbulence in coronal loops: A hybrid shell model. Phys. Rev. Lett. **92**, 194501 (2004)
30. NIST, SEMATECH: (2000). *NIST/SEMATECH e-Handbook of Statistical Methods*, www.itl.nist.gov/div898/handbook
31. Nowick, A.S., Vaysleyb, A.V., Kuskovsky, I.: Universal dielectric response of variously doped CeO_2 ionically conducting ceramics. Phys. Rev. B **58**, 8398–8406 (1998)
32. Parnell, C.E., Jupp, P.E.: Statistical analysis of the energy distribution of nanoflares in the quiet Sun. Astrophys. J. **529**, 554–569 (2000)
33. Pauli, W.: *Die allgemeinen Prinzipien der Wellenmechanik*. in K. Geiger and H. Scheel (eds), p.140 Handbuck der Physik 2nd Edition, Vol. 245 (Berlin Springer, 1933)
34. Peng, C.K., Buldyrev, S.V., Goldberger, A.L., Havlin, S., Mantegna, R.N., Simon, M., Stanley, H.E.: Statistical properties of DNA sequences. Physica A **221**, 180–192 (1995)
35. Penrose, O.: An asymmetric world. Nature **438**, 919 (2005)
36. Rundle, J.B., Turcotte, D.L., Shcherbakov, R., Klein, W., Sammis, C.: Statistical physics approach to understanding the multiscale dynamics of earthquake fault systems. Rev. Geophys. **41**, 1019 (2003)
37. Russell, E.V., Israeloff, N.E.: Direct observation of molecular cooperativity near the glass transition. Nature **408**, 695–698 (2000)
38. Scafetta, N., West, B.J.: Multiscaling comparative analysis of time series and geophysical phenomena. Complexity **10(4)**, 51–56 (2005)
39. Schrödinger, E.: Space-Time Structure. Cambridge Univ. Press, Cambridge (1985)
40. Schrödinger, E.: Nature and the Greeks. Cambridge Univ. Press, Cambridge 1954; Canto Edition with *Science and Humanism* (1996)
41. Schrödinger, E.: Science and Humanism. Cambridge Univ. Press, Cambridge 1951; Canto Edition with *Nature and the Greeks* (1996)
42. Schrödinger, E.: Mind and Matter. Cambridge Univ. Press, Cambridge 1958; Canto Edition with *Autobiographical Sketches* and *What is Life*, Tenth printing (2003)
43. Suber, P.: A crash course in the mathematics of infinite sets, http://www.earlham.edu/∼peters/writing/infapp.htm, published in the *St. John's Review*, **XLIV**, 2, 35–59 (1998)
44. Szulga, J., Molz, F.: The Weierstrass Mandelbrot process revisited. J. Stat. Phys. **104**, 1317 (2001)
45. Tsallis, C.: Possible generalization of Boltzmann-Gibbs statistics. J. Stat. Phys. **52**, 479–487 (1988)
46. Tsallis, C., Levy, S.V.F., Souza, A.M.C., Maynard, R.: Statistical-mechanical foundation of the ubiquity of Lévy distributions in nature. Phys. Rev. Lett. **75**, 3589–3593 (1995)
47. Tsallis, C., Levy, S.V.F., Souza, A.M.C., Maynard, R.: Statistical-mechanical foundation of the ubiquity of the Lévy distributions in nature. Phys. Rev. Lett. **77**, 5442 (1996)
48. Varotsos, P.: A review and analysis of electromagnetic precursory phenomena. Acta Geophys. Pol. **49**, 1–42 (2001)
49. Varotsos, P., Alexopoulos, K.: Thermodynamics of Point Defects and their Relation with Bulk Properties. North Holland, Amsterdam (1986)
50. Varotsos, P.A.: Is time continuous? arXiv:cond-mat/0605456v1 [cond-mat.other] (18 May 2006)
51. Varotsos, P.A., Sarlis, N.V., Skordas, E.S.: Spatio-temporal complexity aspects on the interrelation between Seismic Electric Signals and seismicity. Practica of Athens Academy **76**, 294–321 (2001)
52. Varotsos, P.A., Sarlis, N.V., Skordas, E.S.: Long-range correlations in the electric signals that precede rupture. Phys. Rev. E **66**, 011902 (2002)
53. Varotsos, P.A., Sarlis, N.V., Skordas, E.S.: Seismic Electric Signals and seismicity: On a tentative interrelation between their spectral content. Acta Geophys. Pol. **50**, 337–354 (2002)
54. Varotsos, P.A., Sarlis, N.V., Skordas, E.S.: Attempt to distinguish electric signals of a dichotomous nature. Phys. Rev. E **68**, 031106 (2003)
55. Varotsos, P.A., Sarlis, N.V., Skordas, E.S.: Long-range correlations in the electric signals that precede rupture: Further investigations. Phys. Rev. E **67**, 021109 (2003)
56. Varotsos, P.A., Sarlis, N.V., Skordas, E.S., Lazaridou, M.S.: Entropy in natural time domain. Phys. Rev. E **70**, 011106 (2004)

57. Varotsos, P.A., Sarlis, N.V., Skordas, E.S., Lazaridou, M.S.: Identifying sudden cardiac death risk and specifying its occurrence time by analyzing electrocardiograms in natural time. Appl. Phys. Lett. **91**, 064106 (2007)
58. Varotsos, P.A., Sarlis, N.V., Skordas, E.S., Lazaridou, M.S.: Fluctuations, under time reversal, of the natural time and the entropy distinguish similar looking electric signals of different dynamics. J. Appl. Phys. **103**, 014906 (2008)
59. Varotsos, P.A., Sarlis, N.V., Skordas, E.S., Tanaka, H.K., Lazaridou, M.S.: Attempt to distinguish long-range temporal correlations from the statistics of the increments by natural time analysis. Phys. Rev. E **74**, 021123 (2006)
60. Varotsos, P.A., Sarlis, N.V., Skordas, E.S., Tanaka, H.K., Lazaridou, M.S.: Entropy of seismic electric signals: Analysis in the natural time under time reversal. Phys. Rev. E **73**, 031114 (2006)
61. Varotsos, P.A., Sarlis, N.V., Tanaka, H.K., Skordas, E.S.: Similarity of fluctuations in correlated systems: The case of seismicity. Phys. Rev. E **72**, 041103 (2005)
62. Varotsos, P.A., Sarlis, N.V., Lazaridou, M.S.: Interconnection of defect parameters and stress-induced electric signals in ionic crystals. Phys. Rev. B **59**, 24–27 (1999)
63. Varotsos, P.A., Sarlis, N.V., Skordas, E.S., Tanaka, H.K.: A plausible explanation of the b-value in the Gutenberg-Richter law from first principles. Proc. Japan Acad., Ser. B **80**, 429–434 (2004)
64. Weiss, J.: Scaling of fracture and faulting of ice on Earth. Surveys in Geophysics **24**, 185–227 (2003)
65. Weron, A., Burnecki, K., Mercik, S., Weron, K.: Complete description of all self-similar models driven by Lévy stable noise. Phys. Rev. E **71**, 016113 (2005)
66. Weron, K., Jurlewicz, A., Jonscher, A.K.: Energy criterion in interacting cluster systems. IEEE Trans. on Dielectrics and Electrical Insulators **8**, 352–358 (2001)
67. Weyl, H.: Space-Time-Matter. Dover, New York (1952)
68. Wigner, E.: On the quantum correction for thermodynamic equilibrium. Phys. Rev. **40**, 749–759 (1932)
69. Wilczek, F.: Nobel lecture: Asymptotic freedom: From paradox to paradigm. Rev. Mod. Phys. **77**, 857–870 (2005)
70. Wilczek, F.: Whence the Force F=ma? III: Cultural Diversity. Physics Today **58(7)**, 10–11 (2005)
71. Yourgrau, P.: A World Without Time:The forgotten legacy of Gödel and Einstein. Basic Books, Cambridge MA (2005)

http://www.springer.com/978-3-642-16448-4

Natural Time Analysis: The New View of Time
Precursory Seismic Electric Signals, Earthquakes and other Complex Time Series
Varotsos, P.; Sarlis, N.V.; Skordas, E.S.
2011, XXIV, 452 p., Hardcover
ISBN: 978-3-642-16448-4